An Adaptive Update Method For A Regenerative Turboshaft Cycle

by

James Bevilacqua

B.S., Aeronautics and Astronautics
Massachusetts Institute of Technology
(1988)

SUBMITTED TO THE DEPARTMENT OF
AERONAUTICS AND ASTRONAUTICS
IN PARTIAL FULFILLMENT OF THE
REQUIREMENTS FOR THE
DEGREE OF
MASTER OF SCIENCE IN AERONAUTICS AND ASTRONAUTICS

at the

MASSACHUSETTS INSTITUTE OF TECHNOLOGY

September 1989

Signature of Author: _____

Department of Aeronautics and Astronautics, September 1989

Certified by: _____

Lena Valavani
Associate Professor, Department of Aeronautics and Astronautics
Thesis Supervisor

Accepted by: _____

Professor Harold Y. Wachman, Chairman
Departmental Graduate Committee

An Adaptive Update Method For A Regenerative Turboshaft Cycle

by

James Bevilacqua

Submitted to the Department of Aeronautics and Astronautics
on August 18, 1989 in partial fulfillment of the
requirements for the Degree of
Master of Science in Aeronautics and Astronautics

ABSTRACT

When a regenerative gas turbine engine deteriorates under field conditions, performance losses can be significant due to an inherent downward bias in the steady-state schedules. Much of the performance loss could be recovered by adapting the steady-state control schedules to the engine condition. This thesis investigates methods of automatically updating the steady-state control schedules to assure that the engine continuously performs at maximum safe operating levels.

Thesis Advisor: Lena Valavani
Associate Professor, Department of Aeronautics and Astronautics

Acknowledgments

I would like to thank my advisor, Lena Valavani, for her timely advice and insight. I would also like to thank the General Electric Company for financial support to perform the work. In particular, I would like to thank Mike Idelchik, Kate Koenig, and especially Wayne Miller at General Electric for invaluable technical support. Finally, I would like to thank my parents for their immense financial and moral support during my five years at MIT.

Contents

List of Figures

List of Tables

Chapter 1

Introduction

A regenerative gas turbine engine with a variable area turbine nozzle (VATN) is being considered for the Army's next generation tank. A standard turboshaft engine cannot meet the Army's vehicle acceleration or specific fuel consumption (sfc) requirements. To meet these requirements a regenerative gas turbine engine with a VATN is necessary. Maximum steady-state efficiency is obtained by maintaining a high operating line. Controlling to a high engine operating line implies controlling the engine at or near its physical limits. If the limiting parameter is not measured (SM, T35, T41, T45), it must be estimated based on measured parameters. For the engine studied in this thesis, the estimation algorithms that are used are open loop schedules. Each schedule maps a limiting cycle parameter into a value of T6 as a function of Np, Ng, and T1.

When the engine deteriorates under field conditions, or in the presence of engine

to engine uncertainty, performance losses can be significant due to the inherent downward bias created by scheduling all engine limits open loop with T6. Much of this performance loss could be recovered by automatically adapting the T6 steady-state control schedules to the engine condition.

This thesis investigates methods of automatically updating the steady-state control schedules to maintain peak performance over the life of the engine. In order to adapt the schedules appropriately the engine condition must be known. Accurately determining the engine and recuperator health given the limited number of measurements available on a production engine is a challenging problem. This is the major analytical portion of this work. Once engine and recuperator health have been determined the T6 schedules can be updated to reflect the specific engine. This allows the engine to regain a significant amount of the performance that is lost due to the deterioration of the engine and recuperator.

1.1 Outline of This Study

The first task is to describe the engine in question and the model of it. A fairly detailed description of the realtime model and its operation is given in Chapter 2. In addition, a summary of the multivariable/multimode control system that has been developed for this engine is presented in Chapter 2. Performance loss is quantified and the need for adaptive updates is then shown. Chapter 3 begins with the goals of the engine diagnostic system. Two approaches were taken and are outlined in

Chapter 3. The first approach is an open loop attempt to quantify engine condition. The second approach is a steady-state iterative procedure which attempts to utilize all of the available information to determine engine health. Chapter 4 compares the numerical results of these two methods. Chapter 5 highlights the chosen algorithm and the main results of this work. Finally, conclusions and recommendations are presented in Chapter 6.

Chapter 2

Problem Description

2.1 Engine Description

The engine model used in this study was developed at the General Electric Company in Lynn, Massachusetts. The model represents a recuperated turboshaft engine intended for the Army's next generation main battle tank. The components from inlet to exhaust are shown in Figure 2.1. Air enters through the inlet where it undergoes a pressure drop through the inlet filter. The air then enters the compression system, which consists of a four-stage axial compressor and a high efficiency centrifugal compressor. This is a regenerative engine so the highly compressed air from the centrifugal compressor is sent through the recuperator where it is preheated by the exhaust gases. The preheated, highly compressed air leaving the recuperator is mixed with fuel and burned in the combustor. The hot gases from the combustor

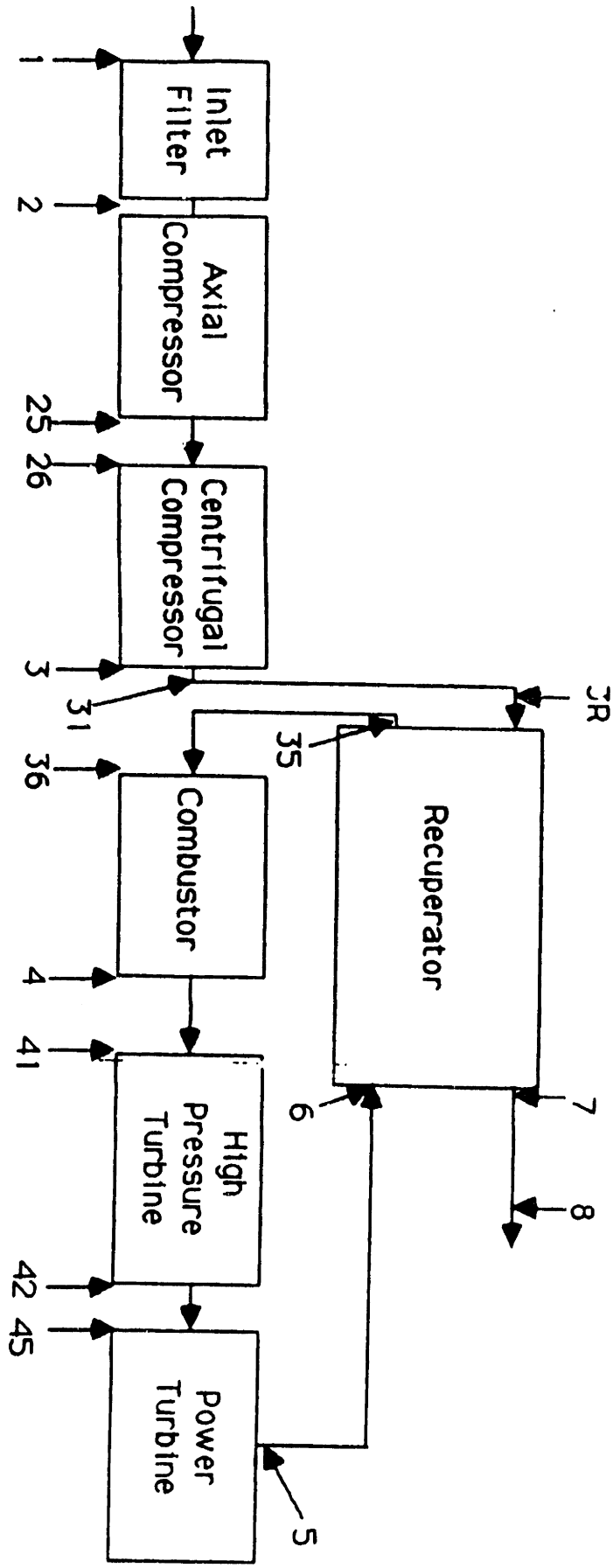

Figure 2.1: Engine Schematic and Station Descriptions

are expanded in the high pressure turbine (HPT), which is on the same shaft as the compressor, producing the horsepower required to drive the compression system and all parasitic horsepower, such as vehicle power extraction and the accessory gearbox. The hot gases are further expanded in the low pressure turbine (LPT), which actually provides horsepower to drive the vehicle. Before the gas is discharged as exhaust, it is fed through the heat exchanger to preheat the air entering the combustor.

This cycle is, of course, a highly nonlinear process. It is further complicated by the fact that turboshaft engines for land-based applications operate over a very wide range. The power turbine is connected to a transmission sprocket which insures large variations in power turbine speed (Np). The large operating range of the engine complicates the engine modeling task and compounds the design of control schedules.

2.1.1 Station Designations

It is conventional to describe the points in the cycle by numbered stations. The station designations are shown in Figure 2.1 and are amplified here.

The engine inlet is designated as station 1. The exit of the inlet filter which is close-coupled to the entrance to the axial compressor is station 2. The exit of the axial compressor is station 25 which then leads to the entrance of the centrifugal compressor, station 26. The centrifugal compressor exit is station 3 which travels down the duct to station 3R, the entrance to the recuperator. Station 36 represents the combustor entrance and the exit of the combustor is designated as station 41. The

HPT exit is station 42 and the LPT entrance station 45. The LPT exit is designated as station 5. The duct from the LPT exit to the recuperator entrance travels from station 5 to station 6. The hot side of the recuperator goes from station 6 to station 7 and the exhaust is designated as station 8.

2.2 Modeling Overview

The nonlinear model used is capable of running in realtime. The realtime constraint imposes a penalty on complexity but, since the model is to be used for control purposes, there must not be a significant loss in accuracy. The model is based on a full blown aero-thermal cycle description which is incapable of running in realtime. However, realtime modeling techniques have advanced to the point where the realtime model provides a very reliable description of the cycle. Increased processor capability and improved modeling have allowed for highly detailed cycle calculations to be computed in realtime. Some of the modeling techniques are:

- Equally spaced table lookups throughout for accuracy and speed.
- Inlet pressure drop and inlet heating included.
- Overall compressor maps modeled with exit flow function and modified with $(\frac{\gamma-1}{\gamma})$ correction; overall stall margin determined from running steady-state full blown model to appropriate axial or centrifugal limit.

- Recuperator counterflow dynamic model utilized for both steady-state and transient operation.
- Simple 10 ms lag used for volume dynamics in recuperator.
- Combustor modeling includes pressure drops.
- Chargeable cooling calculations include appropriate enthalpy effects.
- Power turbine modeled by correlating $\frac{\Delta H}{T45}$ (H45R), corrected speed (XN45R), VATN, and T45.
- Reynolds Number, clearance, and exit swirl effects included in overall power turbine correlation.
- Engine heat soak included in combustor, HPT, and power turbine.

A detailed description of the modeling follows in the next section.

2.3 Detailed Model Description

The overall perspective for this model is a component by component description of the jet engine aero-thermodynamic cycle. The model contains information about each component of the engine and, hence, is modular in nature. Each component is self contained and takes the thermodynamic information at the input (temperature, pressure, flow, enthalpy) and produces the corresponding thermodynamic information

at the exit of the component. It must have sufficient complexity to provide accuracy and sufficient simplicity to be able to process in real time.

Inlet

The incoming air is passed through a filter and as a result undergoes a pressure loss and some heating effects. The inlet pressure loss is calculated as a function of $W2R^2$.

$$P2 = P1(1 - C * W2R^2) \tag{2.1}$$

The constant represents inlet filter losses plus other inlet losses. The inlet heating is simply a univariate function of corrected core speed (PCN2R)

$$T2 = T1 + f(PCN2R) \tag{2.2}$$

and the enthalpy is calculated based on the relationship with temperature for air.

$$H2 = f(T2) \tag{2.3}$$

Axial Compressor

The second component is the axial compressor. It takes the shaft energy provided by the high pressure turbine and, through blade aerodynamics, converts it to pressure energy. The operational characteristics of the axial compressor are generically repre-

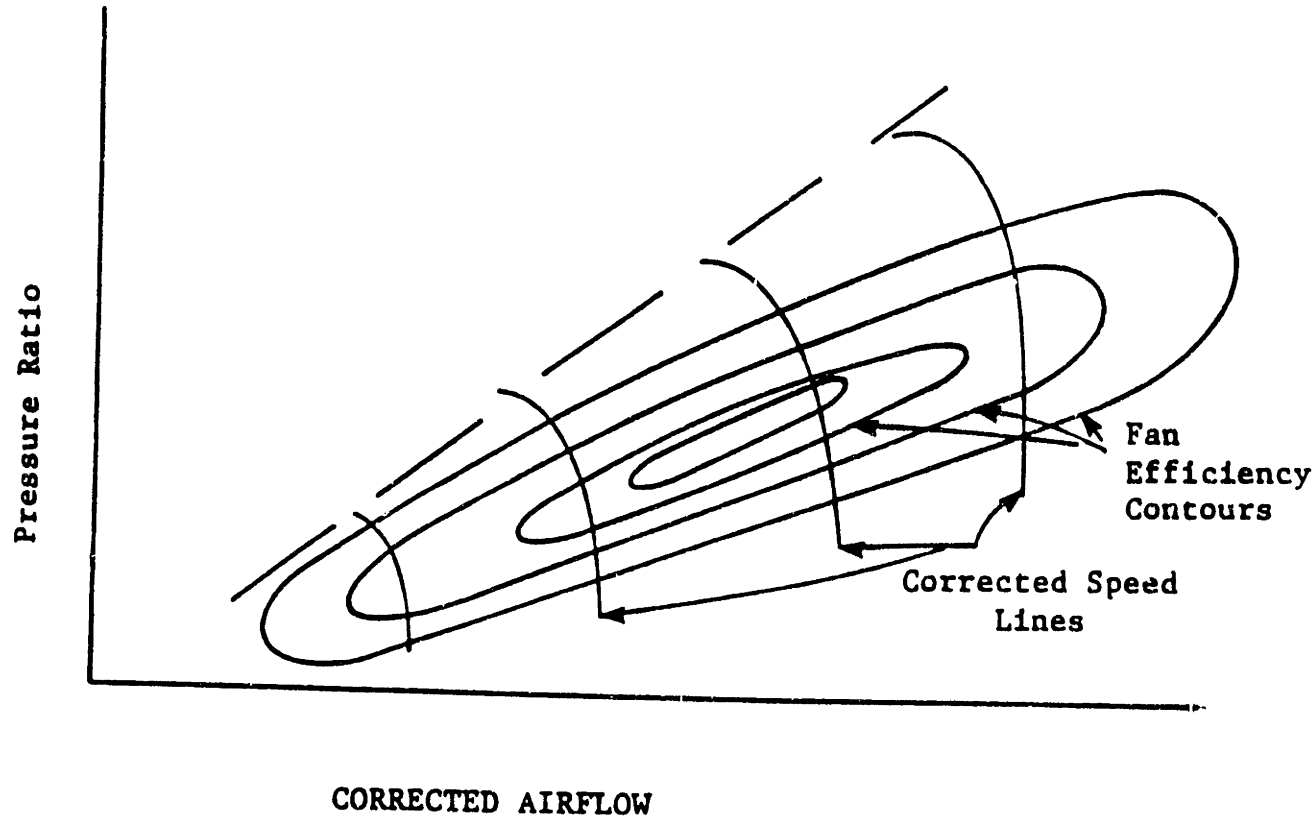

Figure 2.2: Generic Compressor Map

sented by a four-dimensional compressor map, as in Figure 2.2. The figure shows the highly nonlinear relationships between airflow, speed, pressure ratio, and efficiency. The x-axis is corrected airflow, where the correction parametrically collapses performance over a variety of inlet conditions. The correction is a result of dimensional analysis which produces non-dimensional parameters. These corrected parameters collapse performance to remove the variability due to inlet conditions. The definition of corrected airflow is

$$W2R = \frac{W2\sqrt{T2/518.67}}{P2/14.696} = \frac{W2\sqrt{\theta_2}}{\delta_2} \tag{2.4}$$

The y axis is fan pressure ratio. The corrected speed lines and lines of constant efficiency, called efficiency islands, are also shown. Therefore, at a given corrected speed and corrected flow, the pressure ratio is defined for a given efficiency.

By transforming these maps to a function of exit ideal corrected flow in place of inlet corrected flow the map characteristics are compressed and linearized. This new map is shown in Figure 2.3. So for the axial compressor, defining the exit ideal corrected flow as

$$W25R = \frac{W25\sqrt{T25I/518.67}}{P25/14.696} = \frac{W25\sqrt{\theta_{25}}}{\delta_{25}} \tag{2.5}$$

the compressor maps give us the pressure ratio ($\frac{P25}{P2}$) and efficiency (η_{axial}).

$$\frac{P25}{P2} = f(W25R, \frac{Ng}{\sqrt{\theta_2}}) \tag{2.6}$$

$$\eta_{axial} = f(W25R, \frac{Ng}{\sqrt{\theta_2}}) \tag{2.7}$$

At this point modifiers are added to the efficiency and flow values. This is how off nominal or deteriorated performance is represented. For example, an adder of -.02 on η_{axial} would represent deterioration of two points for the axial compressor.

The axial compressor inlet flow is then back calculated based on parameters that have already been calculated at the exit of the axial compressor. Exit ideal temperature (TI25) is all that remains to be calculated at the axial exit because exit pressure

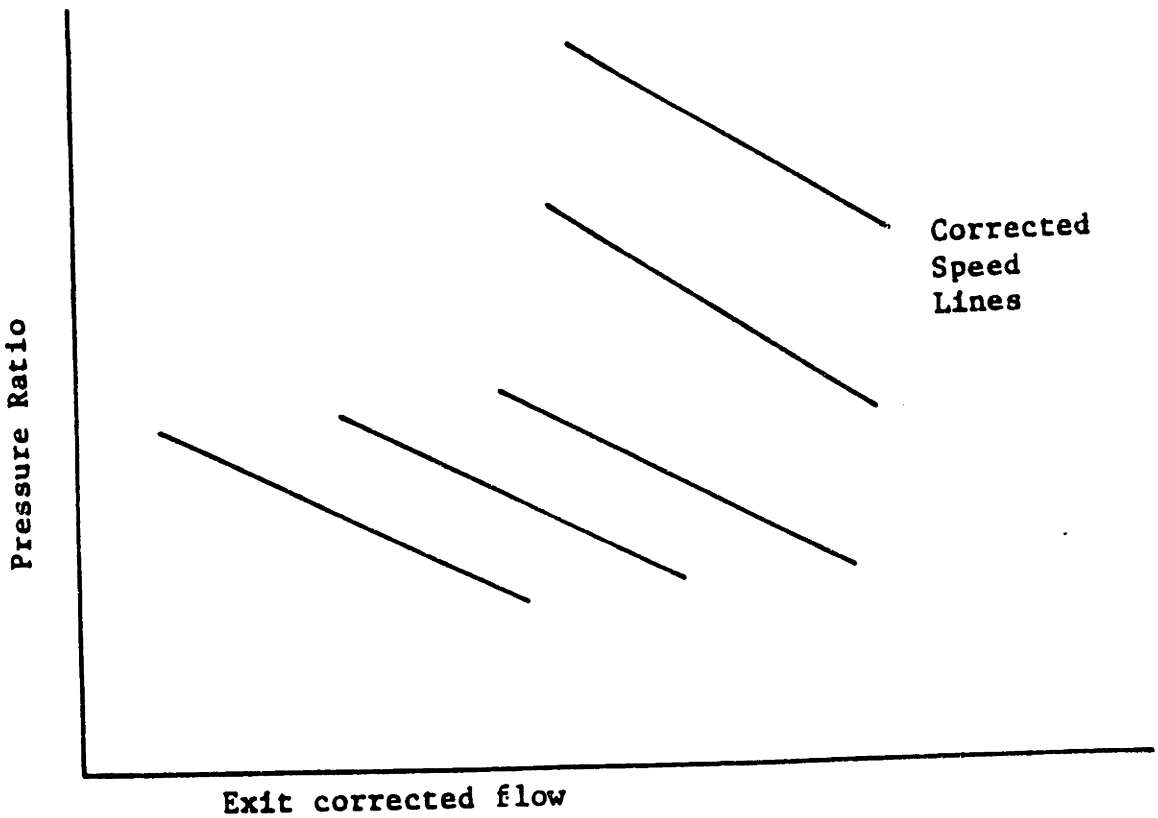

Figure 2.3: Generic Exit Corrected Flow Compressor Map

(Equation 2.6) and exit corrected flow (Equation 2.5) have already been calculated. TI25 is obtained from the relationship with the relative pressure ratio across the axial compressor. Some intrinsic thermodynamic, compressible flow relationships have been put in equally spaced tabular form for use in the model. Two of these are used here to calculate the exit ideal temperature. The relative pressure ratio is obtained from the relationship of relative pressure to temperature for air

$$PREL25 = \frac{P25}{P2} f(T2) \tag{2.8}$$

The exit ideal temperature is then obtained by looking up the reverse relationship of temperature vs relative pressure for air

$$TI25 = f(PREL25) \tag{2.9}$$

Centrifugal compressor inlet airflow can be calculated as a function of exit corrected airflow, pressure ratio and temperature ratio. Since $W25 = W2$, then

$$W2R = \frac{W25R * P25\sqrt{\theta_2}}{\sqrt{TI25}\,\delta_2} \tag{2.10}$$

$$W2 = \frac{W2R * \delta_2}{\sqrt{\theta_2}} \tag{2.11}$$

The calculation of airflow may seem backward here, but there is the necessity to iterate the flow to match continuity requirements. For steady-state points the

iteration is done by multiple passes but, if the model is to be run in realtime, the iteration is done in out in realtime. The iteration scheme will be described fully in Subsection 2.3.2.

Exit ideal enthalpy is found in the table relating enthalpy to temperature for air

$$H25I = f(TI25) \tag{2.12}$$

and then corrected by the efficiency to get the actual enthalpy

$$\Delta H = \frac{(H25I - H2)}{\eta_{axial}} \tag{2.13}$$

$$H25 = H2 + \Delta H \tag{2.14}$$

Finally, exit temperature is obtained from the enthalpy vs. temperature relationship for air

$$T25 = f(H25) \tag{2.15}$$

Several bleed and cooling flows that are taken from the axial compressor are bookkept at this point

$$W26 = W2 - W_{cool} - W_{leak} \tag{2.16}$$

The axial compressor power is computed by the enthalpy change times flow relationship

$$PW2 = W2 * (H25 - H2) * C \tag{2.17}$$

where the constant is a conversion factor to horsepower.

The last thing to be calculated is the stall margin. This is done at flow and is simply read from the compressor map as a function of corrected inlet flow.

Centrifugal Compressor

The next component in the engine is the centrifugal compressor. The modeling is basically identical to that of the axial compressor. The maps are different but the logic flow is the same. We pick up a continuity check matching the corrected flow at the inlet to the centrifugal compressor. The exit corrected flow (FF3I) is guessed at initially and then iterated on. The iteration matches the corrected flow at the inlet that is back calculated from the guess to the one that is calculated based on the flow to that point.

Deterioration of the centrifugal compressor is modeled by adders and scalers on the efficiency and flow. The power calculated for the centrifugal compressor is added to the power that is calculated for the axial compressor to give a total power for the compression system.

$$HPC = PW2 + PW26 \tag{2.18}$$

There are also several bleed and cooling flows which are extracted from the centrifugal compressor which need to be accounted for.

$$W31 = W3 - W_{cool} - W_{leak} \tag{2.19}$$

Generic Pressure Loss Modeling

Throughout the engine there are pressure losses which occur in the ducting from station to station. These are basically all modeled in the same way so only the general case will be described.

In general, at the duct entrance a dimensionless flow function and a γ must be calculated. The thermodynamic tables are used to obtain γ from a function of temperature.

$$\gamma = f(T) \tag{2.20}$$

Another preprogrammed table gives the velocity head as a function of dimensionless flow function and gamma. The velocity head can be thought of as an effective Mach number.

$$Velocity\ Head = \frac{q}{P_{inlet}} = \frac{\frac{1}{2}\rho v^2}{P_{inlet}} = f(FF^2, \gamma) \tag{2.21}$$

For a constant area duct, the value of $\frac{\Delta P}{q}$ is constant. The value of $\frac{\Delta P}{P_{inlet}}$ is not constant, however, and that is why the velocity head is needed. Given the velocity head obtained from the thermodynamic tables, P_{inlet}, and the duct dependent value of $\frac{\Delta P}{q}$, $\frac{\Delta P}{P_{inlet}}$ can then be calculated.

$$\frac{\Delta P}{P_{inlet}} = \frac{\Delta P}{q} * \frac{q}{P_{inlet}} \tag{2.22}$$

And, finally, it is just a matter of manipulation to arrive at the duct exit pressure

$$\frac{P_{exit}}{P_{inlet}} = 1 - \frac{\Delta P}{P_{inlet}} = 1 - \frac{P_{inlet} - P_{exit}}{P_{inlet}} \tag{2.23}$$

where P_{exit} is then just

$$P_{exit} = \frac{P_{exit}}{P_{inlet}} * P_{inlet} \tag{2.24}$$

Ducting From Compressor to Recuperator

A pressure loss is modeled from the exit of the centrifugal compressor to the entrance of the duct leading to the recuperator (station 3 to station 31). At this point, PS31 is calculated since it is a sensed variable. Again, the thermodynamic tables provide the relationship. This time it is the ratio of total pressure to static pressure based on flow function squared and γ

$$\frac{P_{total}}{P_{static}} = f(FF^2, \gamma) \tag{2.25}$$

$$PS31 = P31 * \frac{P_{static}}{P_{total}} \tag{2.26}$$

A pressure loss is modeled in the duct from the compressor to the entrance of the recuperator (station 31 to station 3R). Leakage in the recuperator is a phenomenon that must be detected by our diagnostic system. To model it, flow is taken out of station 3R and put back in at station 6. This effectively takes flow from the high pressure, low temperature side of the recuperator to the lower pressure, higher temperature side of the recuperator. Ideally there would be no leakage but, if there

is, the performance loss is significant. Knowing that the leakage in the recuperator is the cause would be very beneficial for engine field service.

Recuperator

The airflow reaches the recuperator where it is heated by the exhaust flow. The recuperator is actually modeled as a four section cross flow model. For simplicity, the generic equations for a one section model will be described realizing that in actuality it is modeled in four sections. Essentially, the heat transferred to the recuperator tubes from the cold and hot sides during each time step is calculated as

$$Q_c = W_c\, c_{p_c}\,(T3R - T35) = H_c\, A_c\,(T_c - T_m) \tag{2.27}$$

and

$$Q_h = W_h\, c_{p_h}\,(T6 - T7) = H_h\, A_h\,(T_h - T_m) \tag{2.28}$$

where

- Q_c, Q_h = heat transferred to recuperator tubes from cold and hot sides, respectively, during successive time steps
- W_c, W_h = mass flow rates on cold and hot sides of recuperator (W3, W6), respectively
- c_{p_c}, c_{p_h} = average heat capacities of gas on cold and hot sides of recuperator, respectively

- A_c, A_h = heat transfer areas on cold and hot sides of recuperator, respectively
- T_c, T_h = average gas temperatures on cold and hot sides of recuperator, respectively
- H_c, H_h = heat transfer coefficients on cold and hot sides of recuperator, respectively
- T3R = inlet temperature on cold side of recuperator
- T35 = exit temperature on cold side of recuperator
- T6 = inlet temperature on hot side of recuperator
- T7 = exit temperature on hot side of recuperator
- T_m = metal temperature of tubes in recuperator

The metal temperature in the recuperator can then be updated every time step by

$$M_r \, c_{p_r} \frac{dT_m}{dt} = Q_c + Q_h \tag{2.29}$$

or

$$T_{m_{t+1}} = T_{m_t} + \frac{Q_c + Q_h}{M_r \, c_{p_r}} \Delta t \tag{2.30}$$

where

- M_r = mass of recuperator
- c_{p_r} = heat capacity of recuperator

- Δt = time step in transient program

When the model is run transiently, the four metal temperatures are updated explicitly by Equation 2.30. However, if the model is being run to a steady-state point, the four metal temperatures are iterated on to satisfy continuity. Continuity in this instance is based on the fact that, at steady-state, the metal temperature and the air temperature at the same station in the recuperator are the same. The result is that at steady-state the recuperator adds four variables that need to be included in the iteration scheme.

A pressure drop is also modeled in the recuperator. This is calculated based on a preprogrammed relationship with the flow function squared at the entrance to the recuperator (3R)

$$\frac{P35}{P3R} = f(FF3R^2) \tag{2.31}$$

In addition, the large volume of air in the recuperator introduces volume dynamics. The volume dynamics are modeled as a simple 10 millisecond lag on the flow leaving the recuperator. The ducting leaving the recuperator and leading to the combustor (35 to 36) has a representative pressure drop which is modeled in the standard way.

Combustor

Now that the air is preheated and compressed, it enters the combustor, is mixed with fuel and the fuel air mixture is burned. Aerodynamic losses cause a pressure drop, and the burning of the fuel air mixture causes a temperature rise. The pressure drop

is an aerodynamic function, and is modeled as a function of flow function squared at the inlet ($FF36^2$)

$$FF36^2 = \frac{W36^2\, T36}{P36^2} \tag{2.32}$$

$$P4 = P36(1 - C * FF36^2) \tag{2.33}$$

The temperature rise due to the burning of the fuel air mixture is modeled as a function of fuel to air ratio (FAR41) and the enthalpy at station 41 (H41). First, the combustor efficiency (η_b) must be calculated. This is a function of combustor exit pressure (P4), combustor inlet flow (W36), and inlet temperature (T36)

$$\eta_b = f(P4, W36, T36) \tag{2.34}$$

Enthalpy can then be calculated as a function of the combustor efficiency (η_b), fuel heating value (FHV), fuel flow (Wf), and inlet air flow (WA4)

$$H4 = \frac{H36 * WA4 + (\eta_b * FHV + C)\, Wf}{WA4} \tag{2.35}$$

The cooling flows must then be added in with the appropriate enthalpy mix to get the enthalpy at the combustor exit (H41). With H41, the exit temperature can be obtained from the thermodynamic table relating temperature to enthalpy and fuel

to air ratio

$$T41 = f(H41, FAR41) - combustor\ liner\ heat\ soak\ effects \tag{2.36}$$

Short term heat soak effects are modeled in the combustor, high pressure turbine and power turbine. They are all done similarly and will be explained in detail in Subsection 2.6.

High Pressure Turbine

The high pressure turbine consists of a choked nozzle to direct the hot gases onto the turbine blades, which are on a common shaft with the compression system. The high pressure turbine can be modeled with the use of a turbine map. The map, as shown in Figure 2.4, needs two inputs. The first input is a $\Delta H/T_{41}$ term. This value is initially guessed at and then included in the iteration scheme to match continuity at the high pressure turbine exit (station 45). The second input is corrected core speed at station 41 ($\frac{XNg}{\sqrt{T41}}$). The map gives two outputs, the corrected flow function at the nozzle (W41R) and the high pressure turbine efficiency (η_{hpt}). After the map is read, the efficiency and the corrected nozzle flow function are scaled by Reynolds number and clearance effects. In addition, scalers and adders representing component deterioration are applied. Both the flow function and the efficiency can be deteriorated.

The HPT pressure ratio is calculated from ideal work and efficiency and includes dissociation effects. The equally spaced thermodynamic tables are utilized for this

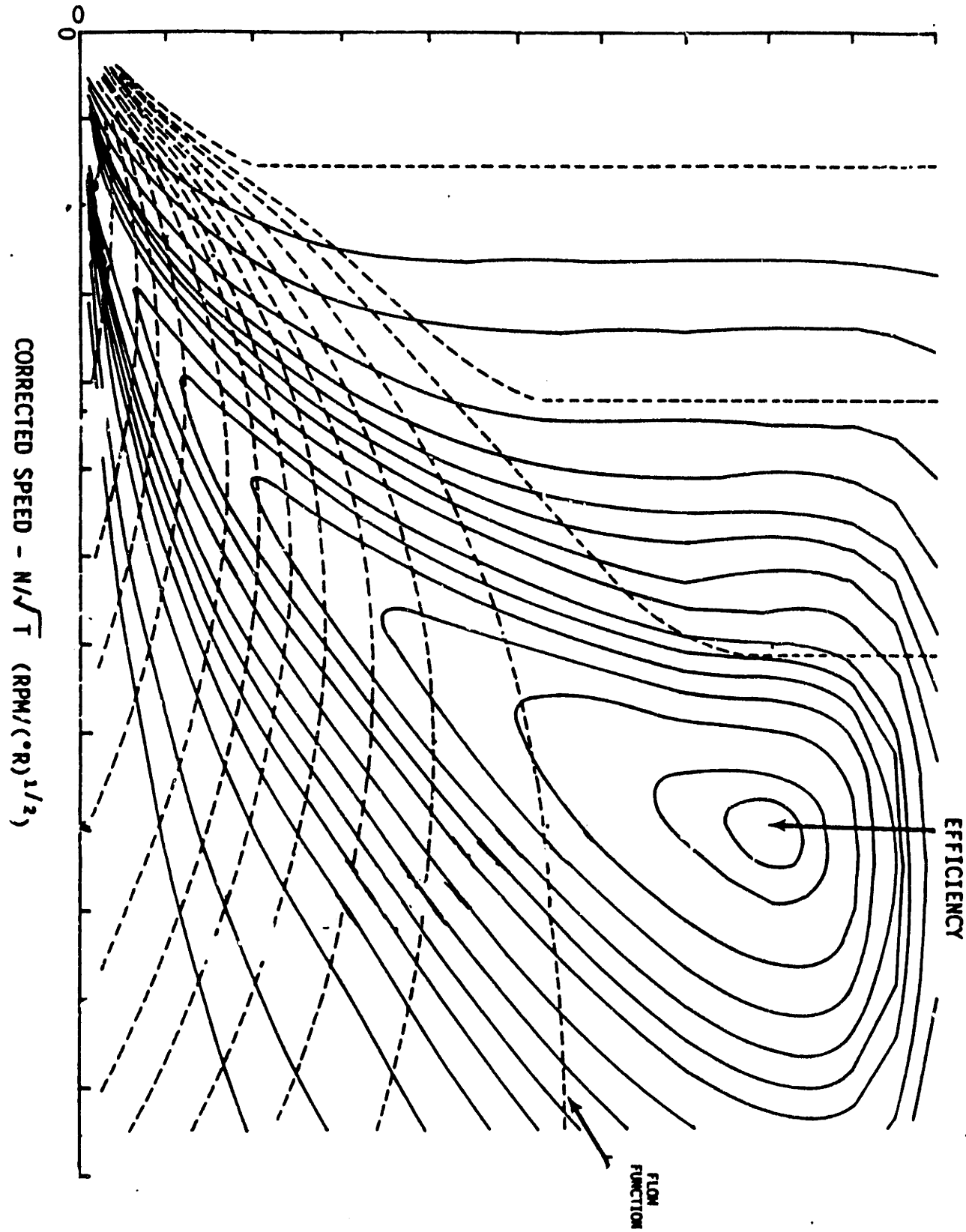

Figure 2.4: Generic Turbine Map

purpose. The short term heat soak for the high pressure tubine is included at this point.

The high pressure turbine power, minus all of the parasitics, must equal the compressor power since they are on the same shaft. The high pressure turbine power (HPHPT) is calculated as a function of enthalpy change and air flow

$$HPHPT = C * WA41\,(H41 - H42) \tag{2.37}$$

From this, a measure of unbalanced horsepower on the high pressure shaft is calculated as

$$UBHPT = HPHPT - HPC - Parasitics - Horsepower\ Extraction \tag{2.38}$$

where the horsepower extraction is the power needed to run the vehicle accessories. In order for the shaft not to break, the unbalanced horsepower must be zero. For steady-state operation of the model, the shaft speed is set so it is included in the iteration scheme. For transient operation, the unbalanced horsepower is used to calculate the explicit update of the gas generator speed.

In addition, another continuity must be satisfied in the high pressure turbine. The flow function that is calculated by the cycle

$$W41R = \frac{W41\sqrt{T41}}{P41} \tag{2.39}$$

must match the flow function that is obtained from the guess on $\Delta H/T_{41}$ which produces a corrected flow function from the turbine map. This continuity match is also included in the iteration scheme.

The high pressure turbine has several chargeable cooling flows which enter before the turbine exit (station 45). The enthalpy at station 45 (H45) is calculated from the enthalpy mix of all of the cooling flows and the main flow. High pressure turbine exit temperature is obtained from the thermodynamic relationship between enthalpy, fuel to air ratio, and temperature

$$T45 = f(H45, FAR45) \tag{2.40}$$

An interturbine pressure loss is a function of flow function squared

$$P45 = P42 * f(FF42^2) \tag{2.41}$$

Power Turbine

The power turbine further expands the hot gases to extract energy to drive the vehicle. The power turbine is modeled as a correlation with $\Delta H/T45$, which is initially guessed at and then iterated on, corrected power turbine speed ($\frac{XNp}{\sqrt{T45}}$), VATN, and T45. The correlation produces the pressure ratio (P45/P49) and the power turbine flow function

$$FF45 = f(\frac{\Delta H}{T45}, \frac{XNp}{\sqrt{T45}}, VATN, T45) \tag{2.42}$$

$$\frac{P45}{P49} = f(\frac{\Delta H}{T45}, \frac{XNp}{\sqrt{T45}}, VATN, T45) \tag{2.43}$$

Continuity at the power turbine nozzle is maintained by including another term in the iteration scheme. The nozzle flow function squared ($FF45^2$) can be calculated based upon parameters that have been calculated thus far:

$$FF45^2_{cycle} = \frac{W45^2 * T45}{P45^2} \tag{2.44}$$

This must match the nozzle flow function squared that is obtained from the correlation based on the guess of $\Delta H/T45$.

The exit enthalpy is obtained based on the inlet enthalpy and the $\Delta H/T45$ that is obtained from the iteration scheme

$$H49 = H45 - \frac{\Delta H}{T45} T45 \tag{2.45}$$

For the purposes of this study a power turbine efficiency calculation was included so deterioration could be modeled

$$\eta_{lpt} = \frac{T45 - T49}{T45(1 - (\frac{P49}{P45})^{\frac{\gamma-1}{\gamma}})} \tag{2.46}$$

The power turbine also has a short term heat soak and chargeable cooling flows which need to be bookkept at this point. Exit flow (W5) and exit temperature (T5) are calculated from the enthalpy mix with the power turbine chargeable cooling flows.

The horsepower is calculated in the same manner as the high pressure turbine

$$HPLPT = C * WA45(H45 - H49) \tag{2.47}$$

Exit Ducting

The duct leading from the power turbine exit has a representative pressure loss. This is not modeled in the standard way but is a function of corrected turbine speed ($\frac{XNp}{\sqrt{T45}}$) and exit flow function (FF5)

$$\frac{P6}{P5} = f(\frac{XNp}{\sqrt{T45}}, \frac{W5\sqrt{T5}}{P5}) \tag{2.48}$$

There is also a temperature loss in the duct which is a function of the ambient temperature and air flow

$$T6 = T5 - C * \frac{T5 - T_{amb}}{W5} \tag{2.49}$$

T6 is a measured variable and is, in fact, the variable which is controlled. The thermocouple lag is modeled as a function of airflow

$$\tau_{T6} = f(W6) \tag{2.50}$$

where τ_{T6} is the time constant.

T7 is the recuperator exit temperature. Since the recuperator is modeled in four stages, T7 is calculated in four stages. The four recuperator metal temperatures are included in the iteration scheme to drive the four metal temperatures to the four flow temperatures in steady-state.

If there is recuperator leakage, the flow is added in after station 6 with the appropriate enthalpy mix. There are duct losses leading to the exhaust (station 7 to 8) which are dealt with in the standard way. There is one last continuity which must be satisfied, and that is a static pressure balance at the exhaust.

A summary of the flow of information from inlet to exhaust is shown in Figure 2.5. The critical parameters for each component are calculated and passed on to the next component. Two things are left which need to be discussed; the short term heat soak modeling, and the iteration scheme.

2.3.1 Short Term Heat Soak Modeling

Short term heat soak effects are included in the combustor, high pressure turbine, and power turbine. Heat soak modeling is added to better match the transient response of the model to the actual engine. Heat soak in the engine is a reflection of the non-adiabatic processes occurring in the engine. This is most dramatic in the high pressure turbine, where the temperature gradient from the hot gas to the metal may be as much as 1000 deg. A lumped parameter estimate of the heat storage in each component is used. The alternative to this approach is an elaborate bookkeeping of

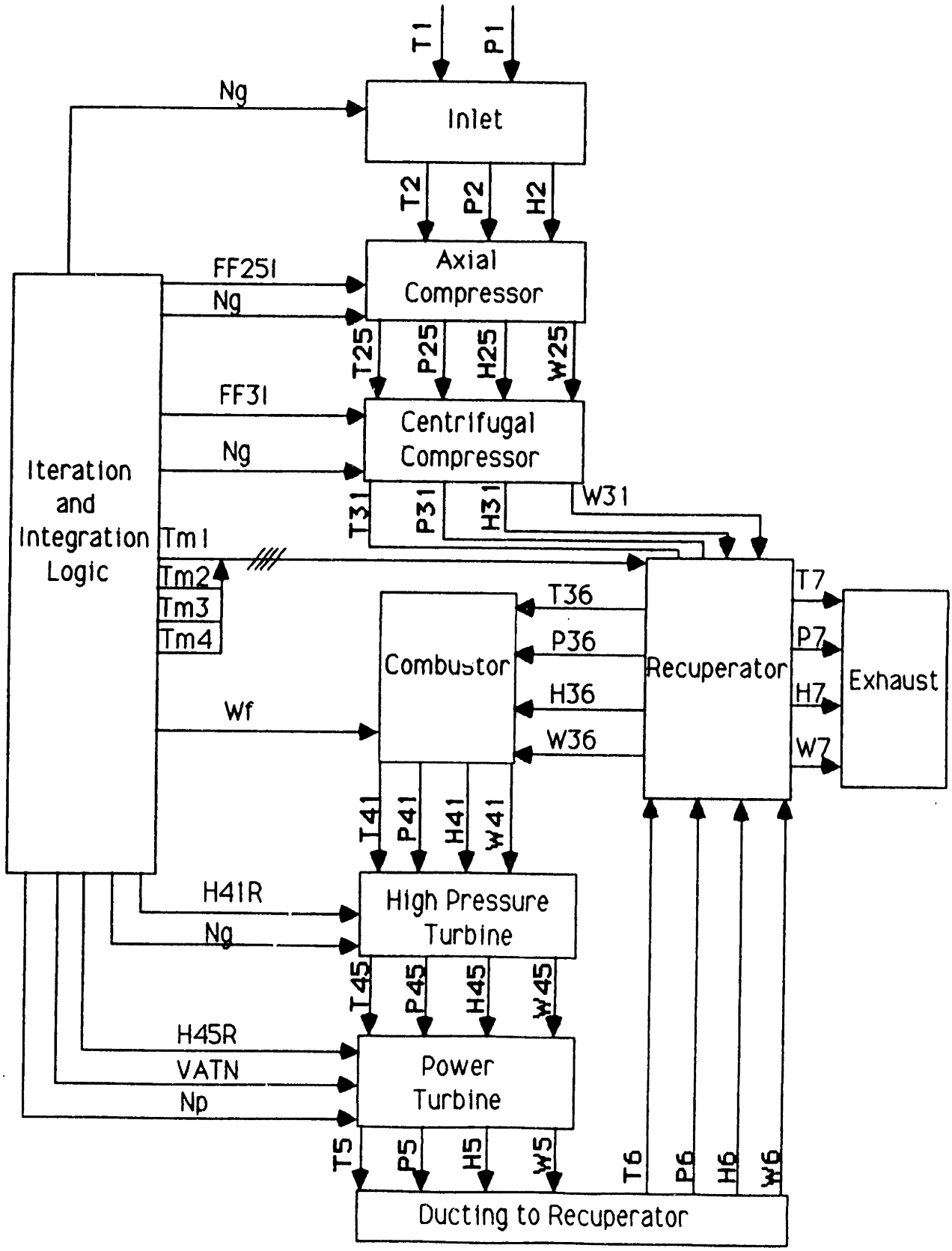

Figure 2.5: Flow of Information in Model

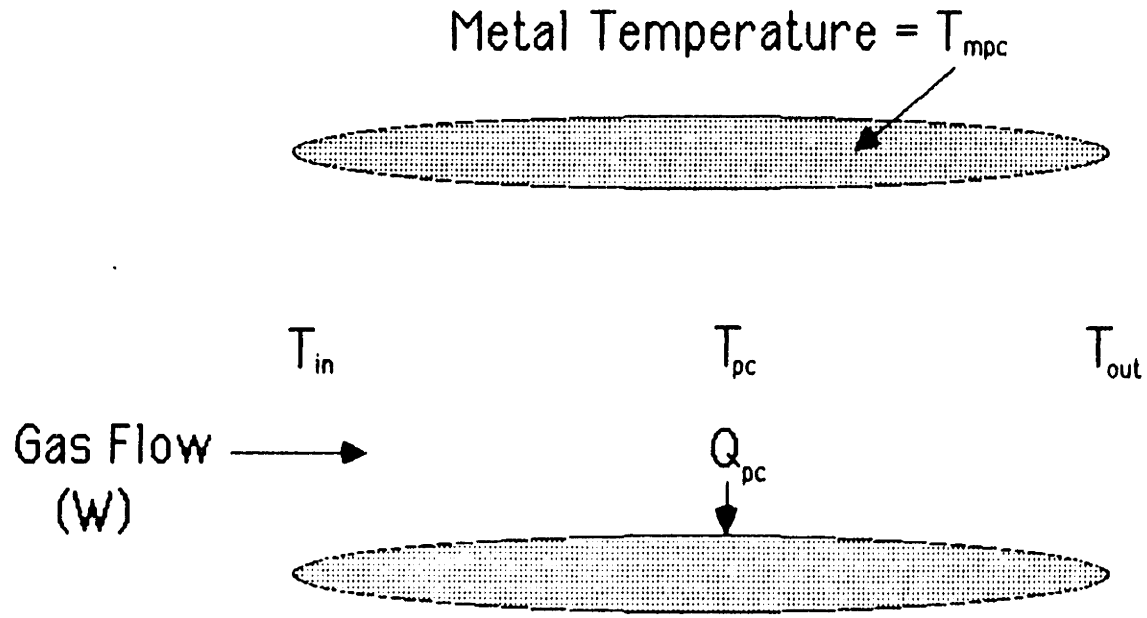

Figure 2.6: Generic Component

all parts exposed to the gas path. The lumped parameter model was generated by analyzing data and comparing it to adiabatic models. The general form is derived from simple heat transfer.

Figure 2.6 represents a generic component. There are three heat transfers that need to be considered. The heat transferred away from the gas stream is

$$Q_{pc} = W\, c_p\, (T_{out_a} - T_{out}) \tag{2.51}$$

or

$$T_{out} = T_{out_a} - \frac{Q_{pc}}{W\, c_p} \tag{2.52}$$

Where T_{out_a} is the adiabatic exit temperature and T_{out} is the actual exit temperature.

The convective heat transferred to the metal is

$$Q_{pc} = H * A\,(T_{pc} - T_{mpc}) \tag{2.53}$$

where

$$T_{pc} = \frac{1}{2}(T_{in} + T_{out}) \tag{2.54}$$

And the convective heat transferred within the metal is

$$Q_{pc} = M * C\,\frac{dT_{mpc}}{dt} \tag{2.55}$$

These three effects reduce to:

$$T_{pc} = \frac{T_{in} + T_{out_a} + C_1\,T_{mpc}}{2 + C_1} \tag{2.56}$$

$$T_{out} = C_2\,T_{pc} - T_{in} \tag{2.57}$$

$$Q_{pc} = C_2\,W\,(T_{pc} - T_{mpc}) \tag{2.58}$$

which are done in each appropriate routine. The integration is done in the time integration section and involves

$$T_{mpc} = T_{mpc} + C_3\,Q_{pc}\,\Delta t \tag{2.59}$$

Iterated Variable	Iterated to Satisfy
Axial Exit Ideal Flow Function (FF25I)	Continuity of flow function at centrifugal entrance (26)
Centrifugal Exit Ideal Flow Function (FF3I)	Continuity of flow function at HPT entrance (41)
ΔH/ T41 (H41R)	Continuity of flow function at power turbine entrance (45)
ΔH/T45 (H45R)	Static pressure balance at exhaust plane (8)
Fuel Flow (Wf)	Zero unbalanced horsepower on the gas generator shaft (UBLPT=0)
Variable Area Turbine Nozzle (VATN)	Engine thermodynamic limits (SM,T35,T41,T45, or T6)
Gas Generator Speed (XNg)	Requested Power Level Angle (PLA)
Power Turbine Speed (XNp)	Requested Power Turbine Speed
Recuperator Metal Temperature #1 (TMCUP1)	Temperature continuity of flow and metal at station 1 in recuperator
Recuperator Metal Temperature #2 (TMCUP2)	Temperature continuity of flow and metal at station 2 in recuperator
Recuperator Metal Temperature #3 (TMCUP3)	Temperature continuity of flow and metal at station 3 in recuperator
Recuperator Metal Temperature #4 (TMCUP4)	Temperature continuity of flow and metal at station 4 in recuperator

Table 2.1: Outline of SLAM

for each component.

The constants C_1, C_2, and C_3 are computed for each component based on their respective masses, areas, and c_p's.

2.3.2 Iteration Scheme

The engine model needs to be solved iteratively to satisfy the continuity requirements outlined in the detailed model description. The iteration is done by a Newton-Raphson procedure until the error terms are within a certain prespecified tolerance

in steady-state. For convenience, this iterative procedure is abbreviated SLAM for Simultaneous Linear Algebraic Method.

For steady-state points the iteration involves twelve elements. They are outlined in Table 2.1.

On the very first pass through the equation set, the initial values of the twelve iterated variables are guessed at. The engine model is run to steady-state initially so the model is iterated with successive passes through this twelve element Newton-Raphson iteration scheme until all of the errors are within a prespecified tolerance.

Once the steady-state point has been solved and we would like the model to run a transient, there are two approaches. The first is by the use of the transient SLAM instead of the steady-state SLAM. Transiently, we need only satisfy the three flow and one pressure continuities. The unbalanced torques and the continuity errors drive the changes in the speeds and recuperator metal temperatures. For example, the gas generator is updated in the following manner:

Since

$$\tau = I\,\alpha \tag{2.60}$$

or

$$\alpha = \frac{dXNg}{dt} = NDOT = \frac{\tau}{I} \tag{2.61}$$

and

$$\tau = C\frac{HP}{XNg} \tag{2.62}$$

where C is a conversion factor. Then NDOT becomes

$$NDOT = \frac{(UBHPT_t - UBHPT_{t-\Delta t})\,C}{XNg\,I} \tag{2.63}$$

or

$$NDOT = \frac{C * UBHPT}{XJg * XNg} \tag{2.64}$$

where XJg is the polar moment of inertia and $UBHPT = HPHPT - HPC$ as explained in the previous section. The gas generator is then updated explicitly

$$XNg_t = XNg_{t-1} + NDOT\,\Delta t \tag{2.65}$$

and is driven by the unbalanced horsepower on the shaft. The power turbine is updated in a similar manner except the load is provided either by a transmission or a dynamometer which is matched at steady-state.

For transient operation, the fuel flow and VATN are provided by the control system. The four recuperator metal temperatures are updated explicitly based on the heat flux at each station. The four remaining elements are solved by a four element SLAM involving only the flow and exit pressure continuities. This method does **not** run in realtime, as the four element SLAM may take several passes to solve, although in general it does not.

To run the model in realtime the Newton-Raphson derivatives are precomputed for the operating envelope and are preprogrammed into the model. At any specific

operating point, the matrix of derivatives is relatively constant. This matrix can be precomputed and used to update the four continuities. Since multiple passes through the iteration scheme would preclude the possibility of running in realtime, only one pass is allowed. Therefore, in each time step, there may be a small error in the continuity errors, but they are forced to be small by the precast derivatives. Preprogramming the derivatives saves the time of computing them each time step. This feature affords the model the capability of running in realtime.

To summarize the iteration scheme, for any operation, a steady-state point must be initially solved. This involves the solution of a twelve element SLAM outlined in Table 2.1. Once solved, the cycle is at steady-state which means:

- balanced horsepower on the shafts
- metal temperature is equal to flow temperature un the recuperator
- the engine is operating at some thermodynamic limit (SM,T35,T41,T45, or T6)
- the engine is operating at some desired power level setting
- the fundamental requirement of continuity of flow throughout and exit static pressure balance is satisfied

To run a transient, not in realtime, a four element SLAM must be solved which involves just the three flow continuities and the exit static pressure balance. This is called the transient SLAM. The speeds and recuperator metal temperatures are updated explicitly, and the fuel flow and VATN are set by the control system.

To run a transient in realtime, the iteration is done in time and not by successive passes. The three flow continuities and the exit static pressure balance are updated by preprogrammed derivatives over the operating range. The speeds and recuperator metal temperatures are updated explicitly. The fuel flow and VATN are set by the control system as in the case of running with the transient SLAM.

It is important to understand the concepts involved here, especially with the steady-state SLAM. The second method used to determine engine condition builds on this by adding elements to the SLAM to monitor the steady-state condition of the engine.

This concludes the description of the modeling of the engine. The next section gives a basic overview of the multivariable/multimode control system that has been designed for this engine.

2.4 Control System Summary

The description of the multivariable/multimode controller is taken primarily from [KM88]. An understanding of the control system is necessary to comprehend the approach taken to automatically update the control system schedules.

For maximum steady-state cycle efficiency the engine must operate at its physical limits. The thermodynamic engine limits encountered are compressor stall margin, combustor inlet temperature (T35), high pressure turbine inlet temperature (T41), power turbine inlet temperature (T45), and recuperator inlet temperature (T6). It is

cost prohibitive to add sensors for each limiting parameter; so the control must protect all the limits by direct control of one measured cycle parameter only. In addition, these engine limits vary as a function of Ng, Np, and ambient conditions. Figure 2.7 illustrates how the engine limits vary over the operating range of the engine.

Previous control mode studies [KM87] have indicated that the thermodynamic cycle limits (SM, T35, T41, T45, T6) can be mapped into T6 for a given operating condition. This decision is well supported by cost and maintainability considerations. The T6 thermocouples are easily accessable and only one gas path temperature is necessary.

Extensive cycle studies were done to establish regions for all of the limiting thermodynamic parameters and to map them into T6. The structure of generating the T6 schedule and the results are shown in Figure 2.8. Note that each map is a four dimensional table which maps cycle limits into the T6 schedule, for instance

$$T6(T35) = f(Ng, Np, T1) \tag{2.66}$$

The ideal control capability provides a means of running the engine model to these cycle limits on a transient or steady-state basis. The T6 schedule was generated with the ideal control defined to protect compressor stall margin (SM), combustor inlet temperature (T35), high pressure turbine inlet temperature (T41), and low pressure turbine inlet temperature (T45).

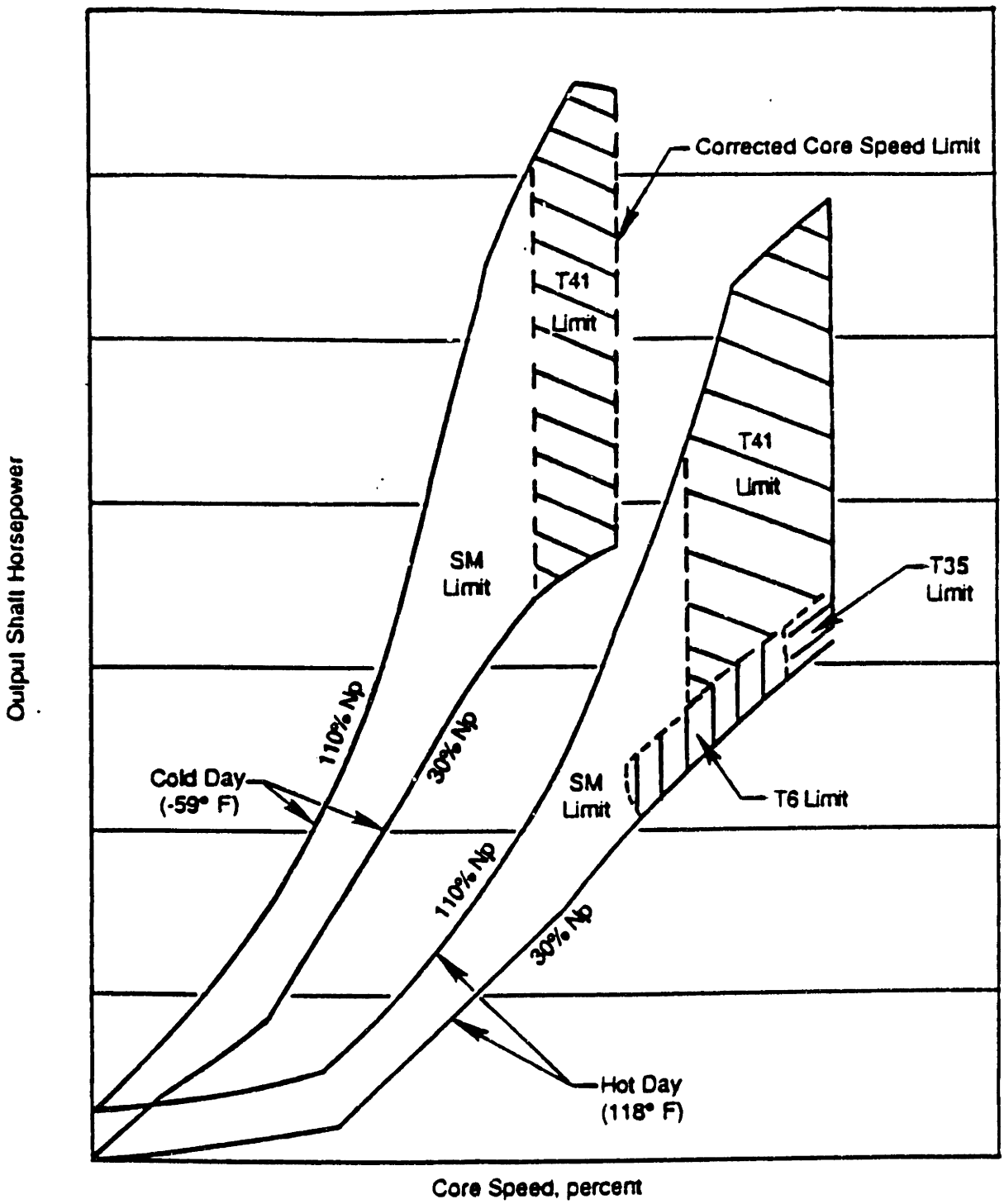

Figure 2.7: Thermodynamic Limits in the Steady-State Operating Regime.

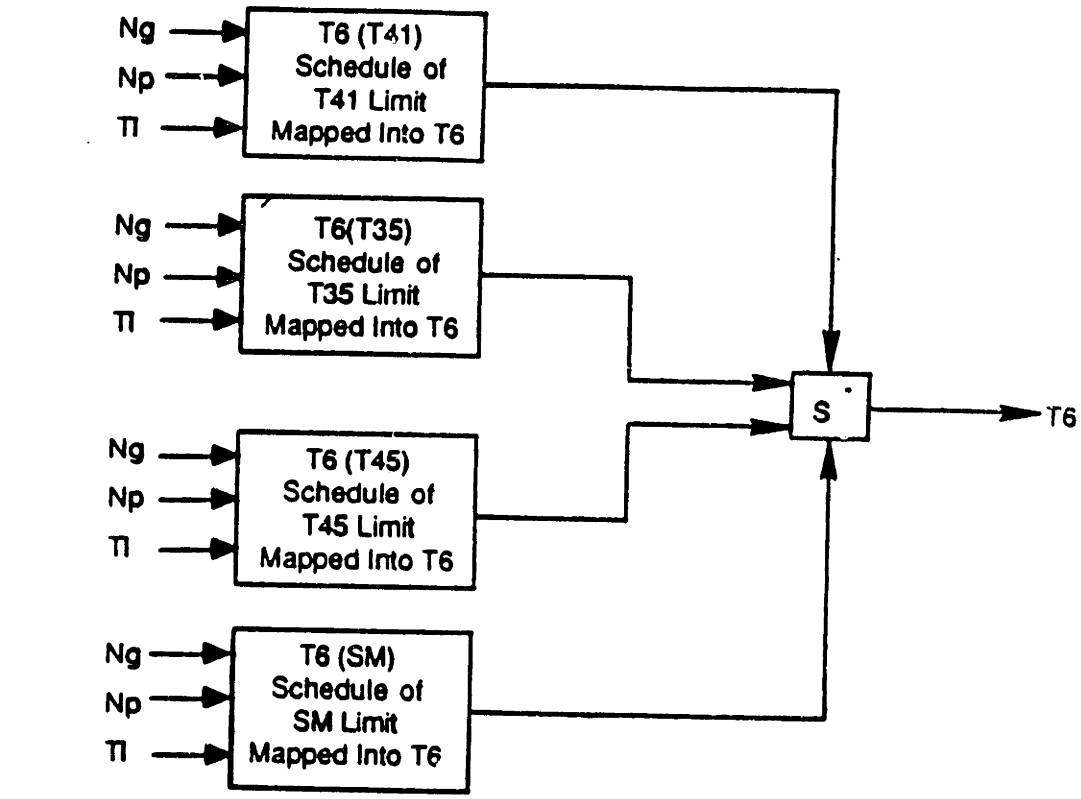

(a) Structure of T6 Schedule

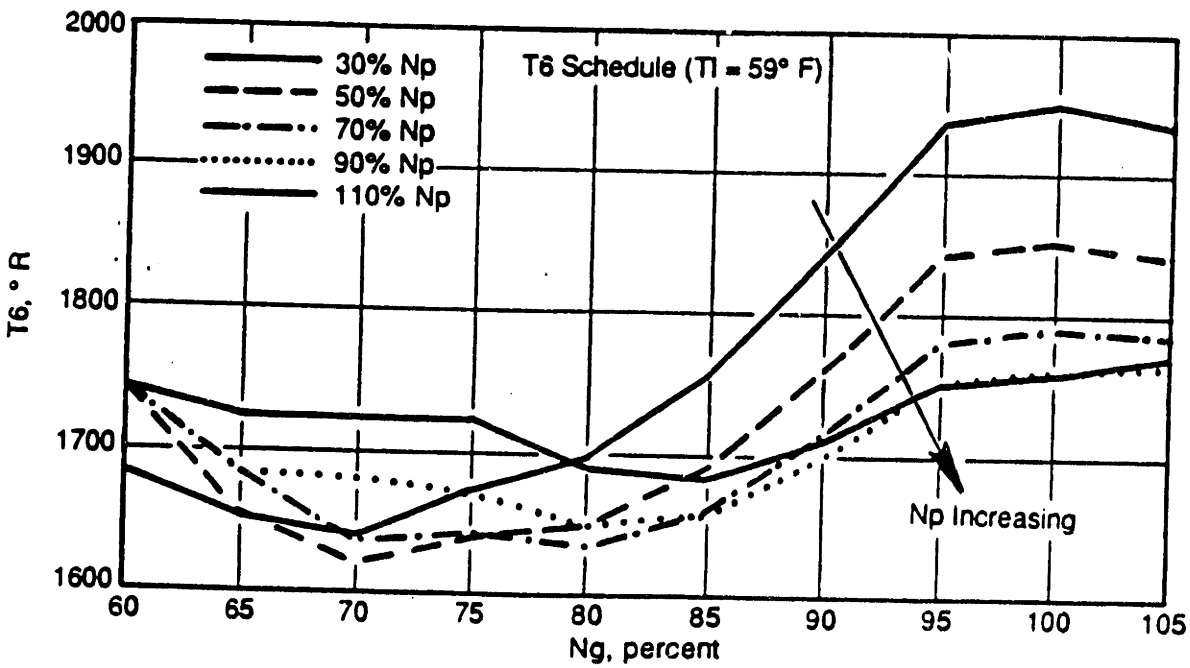

(b) Sea Level Standard Day T6 Schedule

Figure 2.8: Structure of T6 Schedule and Sea Level Standard Day T6 Schedule.

Control Objective	Control Mode	Actuator
Power Modulation	Ng/T6	Wf/VATN
Engine Limits	Ng Top/T6	Wf/VATN
	Np Top/T6	Wf/VATN
	Ng Bot/T6	Wf/VATN
(GE/I or N/I)	Np Bot/T6	Wf/VATN
Engine Acceleration	dNg/dt	Wf

Table 2.2: Multivariable/Multimode Control Modes Summary

2.4.1 Controlled Outputs and Control Variables

The independent inputs which uniquely describe a steady-state cycle point can be divided into two sets. The first set includes ambient conditions; total inlet temperature (T1), and total inlet pressure (P_{t1}). The second set includes active inputs; fuel flow (Wf), variable area turbine nozzle (VATN), compressor variable geometry (CVG), and power turbine load. Power turbine load is a function of transmission gear ratio and grade and is not a control input. Steady-state CVG is scheduled as a function of corrected core speed to optimize compressor performance. The two remaining independent control inputs are Wf and VATN, implying that two cycle outputs may be controlled independently.

2.4.2 Steady-State Control Strategy

Steady-state control strategy was defined in [KM88]. A brief summary of the major control modes follows. In the power modulation region (above idle and below maximum rotor speeds), the controlled cycle parameters are Ng and T6. Np is not controlled and is allowed to float. The Ng reference is scheduled as a function of

power level angle (PLA) to provide linear power modulation. Conversely, at neutral idle (N/I), gear engaged idle (GE/I), and maximum power turbine speed, Np and T6 are controlled and Ng is allowed to float. A summary of all control modes can be found in Table 2.2.

2.4.3 Power Modulation Loop Design (Ng-T6 Loop)

The main operating mode is the Ng-T6 power modulation mode. Initially, a decoupled Ng-T6 design seemed desirable. The difficulty with this is that although the gas generator speed is being controlled, power turbine speed determines vehicle acceleration. Opening the VATN will quickly spool-up the gas generator, but at the expense of the power turbine. Therefore, to minimize vehicle hesitation, a multivariable control system was designed which coordinates fuel flow with VATN to avoid power turbine droop during acceleration.

2.4.4 Gas Generator Acceleration Schedule

Engine acceleration must be limited to maintain transient engine thermodynamic cycle limits (SM, T35, T41, T45). Two traditional ways of accomplishing this are a fuel flow over compressor exit pressure ratio (Wf/PS3) limiter and controlling gas generator acceleration (NDOT) directly. The recuperator heat transfer to the compressor inlet is equivalent to additional fuel flow and, hence, the Wf/PS3 schedule would need to be corrected with T35. In addition, land based vehicles must be able to run on

different fuels with a variety of heating values and again the Wf/PS3 would need to account for this. NDOT does not have any of these drawbacks, therefore NDOT acceleration was chosen rather than Wf/PS3. The NDOT schedule is a function of Np, Ng, T1 and VATN position. When the VATN is open from its steady-state position, a faster acceleration is possible because the engine operating line drops.

2.4.5 Np-T6 Topping and Bottoming Governors

The Np-T6 topping governor is designed to use Wf and VATN to prevent power turbine speed from exceeding maximum speed and maintain T6 at its scheduled level. It is designed as two single-input/single-output (SISO) loops with state feedback. Fuel is modulated based on Np error, and T6 controls only the VATN. Both Np and T6 errors also use Ng state feedback. The bandwidth of the Np topping is limited by a nonminimum phase transmission zero at 1 rad/sec and the large inertia of the power turbine. Due to core acceleration requirements, the Np topping governor is kept out of the way until Np gets within 7% of reference. The governor is not fast enough to keep Np from overshooting, if Np is accelerating quickly, but the overshoot is considered acceptable.

The Np-T6 bottoming governor is designed to keep Np above its bottoming level (near 30%) while maintaining the T6 schedule for optimum sfc. The minimum Np level is set to provide enough power for the parasitic vehicle operations, especially cooling, in idle and gear engaged idle.

2.4.6 Mode Switching Logic

Control mode selection logic for a multimode controller is a well established process for standard turboshaft engines which use only SISO controllers of approximately the same bandwidth. The most limiting control mode is selected based on maximum or minimum fuel flow.

The control mode selection logic for land-based vehicles is complicated by the substantially different bandwidths in the control loops. This is attributable to the different inertias between the gas generator and the loaded power turbine (a ratio of about 10 to 1). Logic is necessary to disable the slow control loops when the engine is not operating near those limits. In addition, selection logic for the fuel and VATN must be coordinated so that the same governor is controlling both inputs. The most limiting fuel flow is chosen by a min/max selection scheme and then the VATN that corresponds to the fuel is used.

2.5 Effects of Deterioration and Leakage on Performance

Although a rotor speed and T6 control may give peak performance for a new, nominal powerpack, maintaining peak performance over the life of the engine is a challenging problem. The performance of the engine is greatly influenced by the T6 reference that is commanded. If the T6 schedules are not modified as the engine and recuperator

deteriorate, significant loss in horsepower can result.

The reference value of T6 is scheduled open loop as a function of gas generator speed (Ng), power turbine speed (Np), and inlet temperature (T2). The optimal value of T6 is obtained by running the engine model with an ideal control. The ideal control has the capability of running the engine to whichever thermodynamic cycle parameter is limiting. The VATN is moved to the point where no thermodynamic limits are violated but the engine is operating at one of them (SM, T35, T41, T45, or T6). T6 is scheduled in this way over the entire operating envelope and the engine is then run to this T6 reference during normal operation. The problem arises when the engine is deteriorated in some way and the open loop schedules no longer place the engine at a thermodynamic limit. The engine could be delivering more power if the T6 schedules were updated so as to properly place the engine at a limit.

To illustrate this point, Figure 2.9 depicts the loss in horsepower that occurs at maximum power with a Ng-T6 control when the engine and recuperator health degrade. The definition of engine deterioration is described in Appendix A. Engine deterioration is on a scale from 0 to 1 with level 1 deterioration representing a fully deteriorated engine. Recuperator leakage is measured as a percentage of flow passing through the recuperator that leaks to the hot side. Leakage goes from 0% to 10%.

Figure 2.9 shows the horsepower loss due to recuperator leakage (x-axis) and engine deterioration (parametrically). What we see is that horsepower loss in temperature limited regions – the high power regime – is certainly significant and will

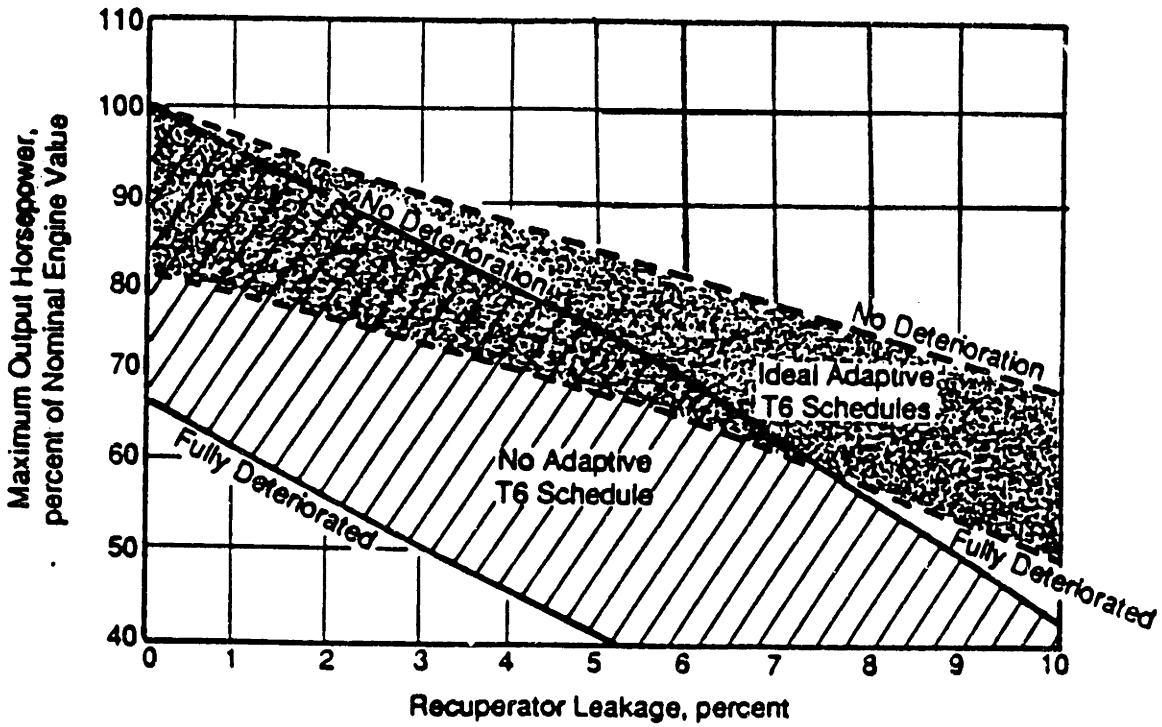

Figure 2.9: Horsepower loss at maximum power can be significantly reduced for current temperature limited cycle by using ideally adaptive T6 schedules.

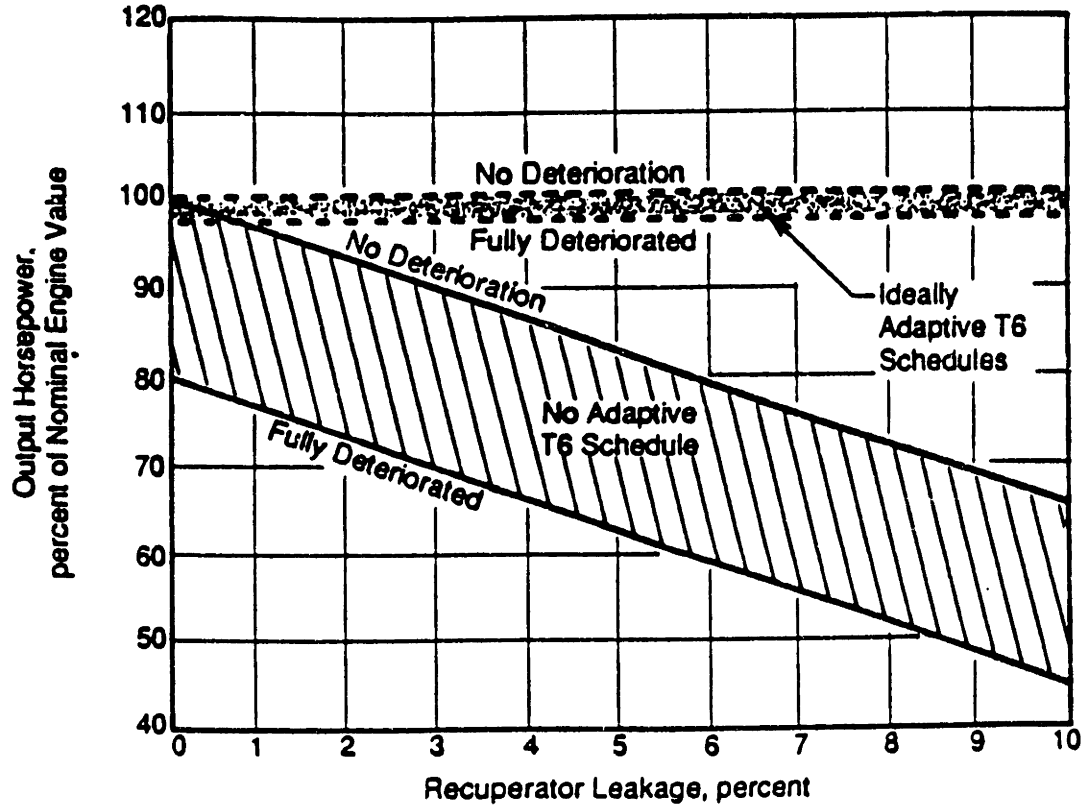

Figure 2.10: Horsepower loss can be eliminated entirely in non-temperature limited regions by using ideally adaptive T6 schedules

cause an unacceptable drop in vehicle performance. With no leakage, a fully deteriorated engine loses over 30% of output horsepower. This number could be reduced to less than 20% with ideally adaptive T6 schedules as Figure 2.9 further shows.

Recuperator leakage effects are worse, as 10% leakage, using the nominal T6 schedules, results in close to 50% loss in output horsepower. With ideally adaptive T6 schedules this could be improved to just a 30% loss. Clearly, it is important to know if the recuperator is leaking so it can be replaced. But more importantly, automatically updating the T6 schedules in an ideal manner in this instance would provide over 25% more output horsepower.

The potential gains are even more impressive in stall limited regimes which include most lower power points. Figure 2.10 shows the effects of recuperator leakage and engine deterioration for a stall limited cycle. With no leakage, a fully deteriorated engine loses 20% of output horsepower using the nominal T6 schedules. Whereas, an ideal adaptive update of the T6 schedules would reduce this loss to less than 3%.

Recuperator leakage of 10% causes a loss of about 35% of output horsepower using the nominal T6 schedules. Ideally adaptive schedules would recover all of the performance loss in this instance.

These two figures show the potential improvements made possible by updating the T6 schedules to match engine and recuperator health. The rest of this thesis deals with how to accomplish this. The update procedure centers around accurately determining engine and recuperator health. If this is done accurately, it is relatively straightforward to update the T6 schedules. Determining engine and recuperator health, given the few measurements available on a production engine, however, is not straightforward and is the focal point of this thesis.

Chapter 3

Engine Diagnostic Algorithms

3.1 Goals of Engine Diagnostic System

The recuperator has been designed so it can be easily replaced in the field if there is a problem. The major problem that could occur with the recuperator is leakage. If the recuperator is leaking, then a percentage of the flow going through it to be preheated will leak straight into the exhaust stream. Engine performance will suffer due to the loss of flow going through the core. So, the primary goal of the engine diagnostic system is to determine if performance loss is due to the recuperator leaking or overall engine deterioration. If the recuperator is causing the problems, it can be replaced in the field.

In addition to separating recuperator effects from engine effects, it is desirable to determine particular component performance levels as well. The control schedules

could be updated more explicitly and, in addition, engine maintenance problems would be simplified. Unfortunately, we are limited in the number of measurements available for analysis. Limited measurements make this task very challenging.

Therefore, the primary goal of the engine diagnostic system is to determine if performance degradation is due to the recuperator leaking or the engine deteriorating. The secondary goal is to break down the overall measure of engine deterioration into individual component performance measures. Once a reliable measure of leakage and/or deterioration has been determined, the T6 schedules can be updated as a function of these parameters.

3.2 Open Loop Algorithm Development

A method was devised that will isolate recuperator leakage from engine deterioration. The idea here is to take a data point of all the available measurements from the engine. This data is then processed through a set of algorithms, based on aero-thermal relationships within the cycle, and a measure of recuperator leakage and engine deterioration is found. The algorithms utilize a sensor set containing only one measurement (PS45) that is not already needed for other powerpack functions.

The set of measurements available for analysis is:

- XNg – Gas Generator Speed (RPM)
- XNp – Power Turbine Speed (RPM)

- T2,P2 – Ambient Inlet Conditions
- T35 – Temperature at Recuperator Cold Side Exit
- T6 – Temperature at Recuperator Hot Side Inlet
- PS31 – Static Pressure at Entrance to Duct Leading to Recuperator Cold Side
- VATN – Variable Area Turbine Nozzle
- XNFPFB – Fuel Pump Speed (RPM)
- Starter/Generator Torque – For Horsepower Extraction (PWX4) Calculation

In addition to these measurements several others were considered. If they could be argued to be advantageous on a cost effective basis, they will be considered for the production engine. They are

- T3 – Temperature at Centrifugal Compressor Exit
- PS45 – Static Pressure at Power Turbine Inlet

The algorithms were developed on the basis of steady state correlations of parameters in the cycle. To do this a study point must be chosen. Gear Engaged Idle (GEI) was chosen as the study point. It was chosen because GEI is a well defined steady-state condition at which the engine will operate. Aerothermal cycle relationships form the basis for the correlations.

3.2.1 Recuperator Leakage

Recuperator leakage is the difference between airflow at the compressor exit (W2) and airflow at the power turbine exit (W6). Compressor inlet flow is obtained from the corrected speed to corrected airflow relationship of the compressor. Flow is then uncorrected using inlet pressure (P2) and temperature (T2). Core horsepower extraction (PWX4) and VATN position are included in the corrected speed/corrected flow relationship in order to reduce operating line variations.

$$W2R = f(\frac{XNg}{\sqrt{\theta_2}}, PWX4, VATN) \tag{3.1}$$

$$W2 = W2R * \frac{\delta_2}{\sqrt{\theta_2}} \tag{3.2}$$

Power turbine exit flow is based upon flow calculations at the power turbine inlet (station 45) because the flow function at the inlet (FF45) is better defined than that at the power turbine exit (station 6). Several correlations for FF45 were attempted and the most effective correlation was found to be with PS45/Pamb and VATN.

$$FF45 = f(\frac{PS45}{Pamb}, VATN) \tag{3.3}$$

This requires the extra measurement PS45 and, unfortunately, no reliable way of calculating FF45 without PS45 could be found. Obtaining W45 from FF45 requires PS45 and T45. So, even if a reliable correlation could be found to obtain FF45 without PS45, PS45 is needed to get W45 from FF45.

T45 must be synthesized, however, and this is done through another correlation. A reliable correlation was found to be the ratio $\frac{T45}{T6}$ as a function of PS45 and VATN. This essentially correlates the temperature ratio across the power turbine ($\frac{T45}{T6}$) to the pressure ratio across the power turbine ($\frac{PS45}{Pamb}$) for varying VATN positions. Other correlations were attempted and were found to be less reliable.

Therefore T45 can be constructed from measured T6, VATN, and PS45.

$$\frac{T45}{T6} = f(\frac{PS45}{Pamb}, VATN) \tag{3.4}$$

$$T45 = \frac{T45}{T6} * T6 \tag{3.5}$$

Flow at the power turbine inlet is then

$$W45 = FF45 * \frac{PS45}{\sqrt{T45}} \tag{3.6}$$

Recuperator leakage can then be calculated as the difference between W2 and W45. However, several cooling flows are extracted after station 2 and replaced after station 45. These would show up as leakage and throw the calculation off significantly. Therefore, these must be bookkept as well and are precalculated based on the nominal cycle operating at gear engaged idle. Leakage, in mass flow rate, is then

$$W_{leak} = W2 - W45 - W_{Chargeable\ Cooling\ Entering\ After\ Station\ 45} \tag{3.7}$$

Since it is convenient to express the leakage in terms of a percentage of flow, this is calculated and is the final expression for recuperator leakage

$$W_{\%leak} = 100 * \frac{W_{leak}}{W2} \tag{3.8}$$

3.2.2 Engine Deterioration Correlation

A measure of overall engine deterioration is obtained via a correlation with the calculated leakage ($W_{\%leak}$), horsepower extraction (PWX4), and VATN.

$$Engdet = f(W_{\%leak}, PWX4, VATN) \tag{3.9}$$

Engdet ranges from 0 to 1 with one representing full deterioration (see Appendix A). The open loop algorithm was limited to overall degradation calculations because attempts to isolate individual component deterioration were not fruitful.

Isolation of Compression System

Attempts to isolate compressor efficiency variations from the overall cycle performance were made. Evaluation of overall compressor efficiency requires knowledge of T3, the exit temperature. Attempts were made to calculate T3 based on the recuperator effectiveness (η_{recup}), T35 and T6 since the recuperator effectiveness is defined as

$$\eta_{recup} = \frac{T3 - T35}{T3 - T6} \tag{3.10}$$

so then T3 can be calculated as

$$T3 = \frac{\eta_{recup} * T6 - T35}{\eta_{recup} - 1} \tag{3.11}$$

However, this calculation is based on a constant recuperator effectiveness. The actual recuperator effectiveness due to heat transfer coefficients is predicited to be constant within 1 – 2 points, but the apparent effectiveness change due to possible recuperator leakage is large, and therefore invalidates the T3 calculation. Small changes in recuperator effectiveness, given T35 and T6 constant, cause large apparent changes in T3, invalidating the calculation of η_{comp}.

Adding a T3 sensor and calculating compressor efficiency directly from Equation 3.12

$$\eta_{comp} = \frac{\frac{PS3}{P2}^{\frac{\gamma-1}{\gamma}} - 1}{\frac{T3}{T2} - 1} \tag{3.12}$$

provides a detection threshold of 2 points with 95% confidence. This information was not considered sufficient to warrant the extra sensor. In addition, a T3 sensor for this application would be very expensive since there is no room at station 3 for a sensor. A major redesign would be required and this information does not warrant such a measure.

Isolation of Turbine System

Attempts to separate the compression system from the turbine system involved calculations of T41. This was abandoned due to the sensitivity to recuperator leakage and the required knowledge of fuel flow. This land based application requires that the engine be able to operate on several different kinds of fuel. Therefore, fuel type is uncertain. So, although volumetric fuel flow can be determined with a low precision error from knowledge of fuel pump speed, mass flow would be uncertain because of fuel type uncertainties. In addition, recuperator leakage effects tended to overwhelm engine deterioration effects when attempting to calculate T41.

3.2.3 Sensors Required for Open Loop Algorithms

The sensors required for the chosen algorithms are Np, Ng, starter/generator torque (for PWX4 calculation), VATN, P2, T2, PS45, and T6. All of these sensors with the exception of PS45 were already considered necessary for other powerpack control and condition monitoring functions. T35, which is available because of engine control requirements, is not needed for these diagnostic algorithms.

3.3 Iterative Diagnostic Algorithm

As Section 4.1 demonstrates, the open loop algorithm results are limited in their usefulness in several ways. Any analysis must be done at GEI and the engine deterioration detection has a wide range. For example, a value of .4 for *Engdet* could

actually have been derived from an actual engine deterioration level of anywhere from .05 – .75. In an effort to improve these results, another method was attempted. This technique involves the 'rubberization'[1] of the engine model by judiciously adding elements to the independent/dependent parameter matrix (SLAM).

The technique is widely used at General Electric for analyzing data obtained during testing in a test cell. It is called Status Cycle Analysis for Test and is abbreviated SCAT. Essentially, independent parameters are added to the twelve element steady state SLAM. These are modifiers to the cycle that represent performance degradation. The corresponding dependent parameters are sensed values that are not already required to define the nominal engine cycle.

The twelve element steady state SLAM defines the equilibrium point. Given the modeling techniques used, all twelve elements are necessary to specify a unique cycle point. In order to rubberize the model extra elements are added to that basic matrix which model performance degradation. Any extra measurements that we have that are not necessary to define the cycle point can then be used as dependent parameters to match up with the cycle modifiers. In effect, we rubberize the engine, through the performance modifiers, until it matches the measurements that we have. By judiciously choosing the modifiers it is hoped that recuperator leakage and engine deterioration can be determined.

The major concept at work here is that the basic twelve element steady-state

[1]Where rubberization implies modifying the basic component performance levels to match the specific engine being monitored

SLAM is all that is needed to define a unique cycle point. However, if deterioration has occured, this solution will be different. It is impossible to determine the level of engine or recuperator degradation with the elements in the basic twelve element SLAM. Therefore, we need additional information to determine what the level of engine or recuperator deterioration actually is for the particular cycle. Any extra measurements that we might have provide additional information. This extra information can be used to more accurately define the particular cycle that is being monitored as follows:

- Tying the extra measurements to a scaler in the cycle that is directly related to the measurement.
- Choosing the best extra measurements to use (T6, T35, PS3, and/or PS45) in order to determine engine deterioration and recuperator leakage.
- Including this measurement/modifier pair in the Newton-Raphson iteration scheme. The calculated cycle value is matched with the measured value by varying the cycle modifier.

Intuition and experience is required to determine what cycle modifier should be tied to what measurement.

SCAT works very well for analyzing test cell data where the engine is heavily instrumented. For example, for just the core test performed in Lynn, a thirteen element SCAT was used to determine pressure losses, efficiencies, flow scalers, etc. throughout the core. The crucial element in getting the SCAT to work well is to

find highly correlated measurements and tie them directly to the scaler or adder that they are correlated to. For instance, a scaler on the pressure loss in the ducting from station 31 to 3R should be well correlated with the pressure measurement at station 3R. Especially if the pressure at station 31 is measured and is tied to the pressure drop in the duct exiting the compressor leading to station 31. Each scaler is allowed to float but is also restricted by the other information available.

The problem with using SCAT on a production engine is the limited availability of measurements to use. The measurements are Ng, Np, P2, T2, and VATN, which are all necessary to define the cycle point so are unavailable for use in SCAT. The extra measurements which are available for use in SCAT are T6, PS3, PS45 (if needed), and T35. PS45 is included for the purposes of this study as a possible measurement although it is not currently planned for the production engine.

The challenge is to develop a SCAT which will reliably determine recuperator leakage and engine deterioration. Several approaches were analyzed and the results appear in Section 4.2.

they are correlated to. For instance, a scaler on the pressure loss in the ducting from station 31 to 3R should be well correlated with the pressure measurement at station 3R. Especially if the pressure at station 31 is measured and is tied to the pressure drop in the duct exiting the compressor leading to station 31. Each scaler is allowed to float but is also restricted by the other information available.

The problem with using SCAT on a production engine is the limited availability of measurements to use. The measurements are Ng, Np, P2, T2, and VATN, which are all necessary to define the cycle point so are unavailable for use in SCAT. The extra measurements which are available for use in SCAT are T6, PS3, PS45 (if needed), and T35. PS45 is included for the purposes of this study as a possible measurement although it is not currently planned for the production engine.

The challenge is to develop a SCAT which will reliably determine recuperator leakage and engine deterioration. Several approaches were analyzed and the results appear in Section 4.2.

The concept behind the SCAT method can be difficult to understand the first time one is exposed to it. It is recommended that the reader reread this section if it is unclear.

Chapter 4

Numerical Results

4.1 Open Loop Algorithms

The algorithms that were chosen and are outlined in Section 3.2 were subjected to a variety of conditions to test their robustness. The results are neatly summarized in Figure 4.1 and Figure 4.2.

The algorithms were tested by inputting variations in inlet temperature, core horsepower extraction, recuperator leakage, and engine deterioration into the model. Calculated recuperator leakage and engine deterioration from the algorithms was compared with the known degradation we are trying to detect.

The x-axis in Figure 4.1 is the actual engine deterioration that was input. The y-axis is the engine deterioration our algorithm produced. The inner band in the graph is due to the variety of inlet conditions such as inlet temperature, core horsepower

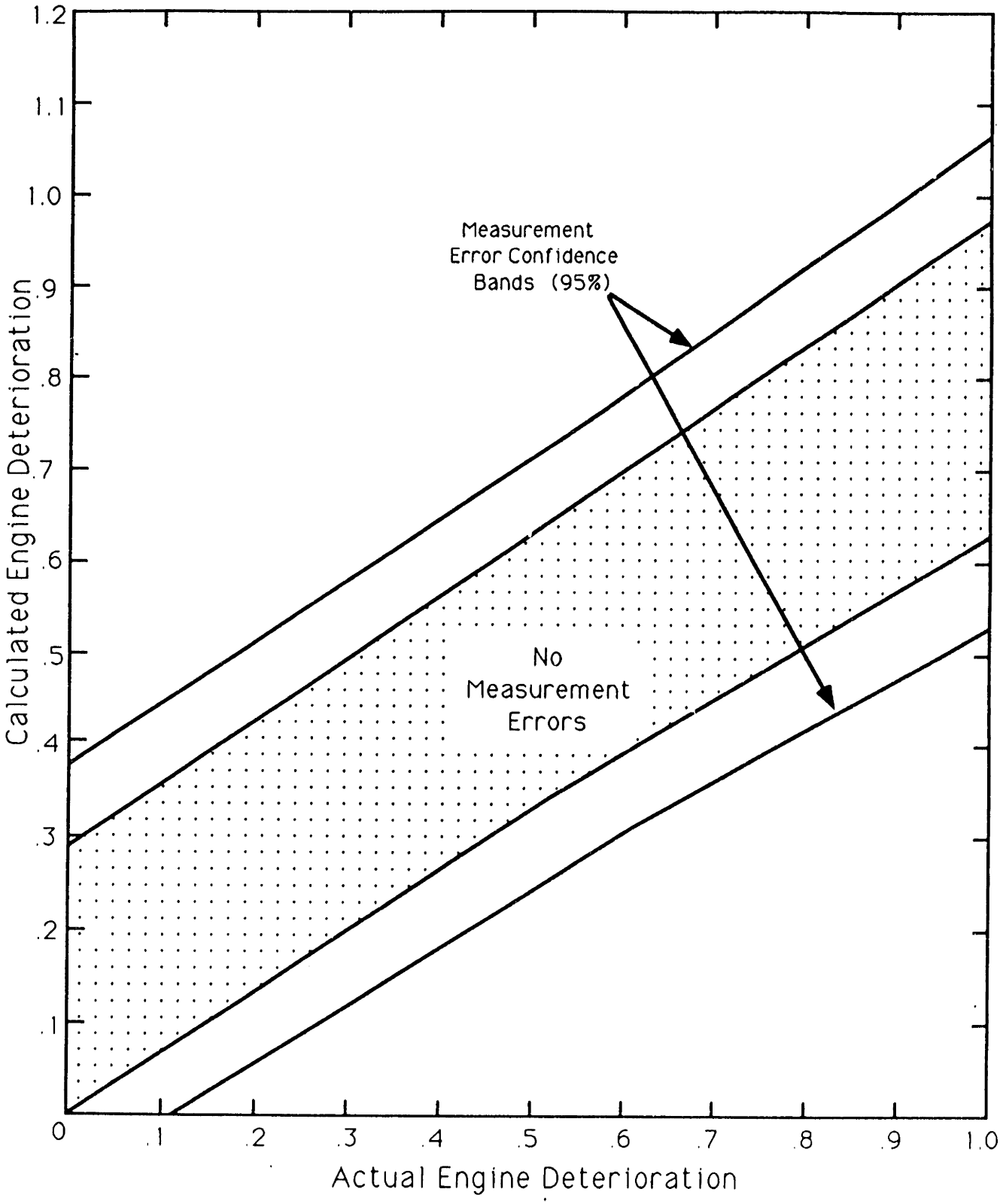

Figure 4.1: Calculated Engine Deterioration vs. Actual Engine Deterioration – Open Loop Algorithms

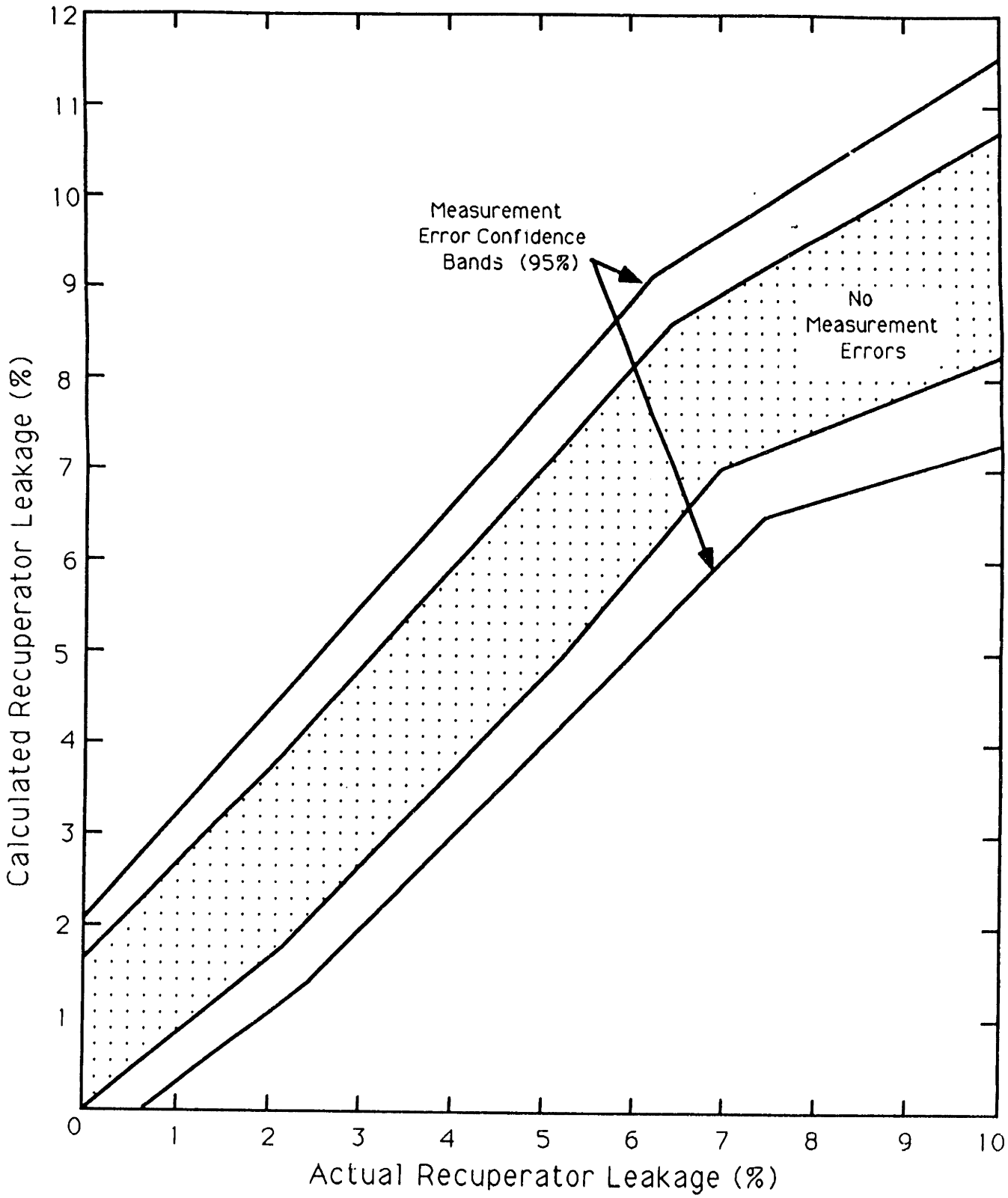

Figure 4.2: Calculated Recuperator Leakage vs. Actual Recuperator Leakage - Open Loop Algorithms

extraction, and recuperator leakage. The outer band is a 95% confidence band. The confidence band was determined for a representative sample of data points by running 500 points per condition with measurement errors imposed. The measurement errors are defined in Appendix B. A Monte Carlo simulator was used to simulate the measurement errors and to generate the data.

The bottom line is that, given uncertainties in

- inlet temperature
- core horsepower extraction
- measurements
- recuperator leakage
- engine deterioration level

the open loop algorithms can detect any leakage with an accuracy of $\pm 1.75\%$ for leakages less than 7% and an accuracy of $\pm 2.3\%$ for leakages greater than 7%. In addition, any engine deterioration will be detected with an accuracy of $+.35/-.1$ for low levels of engine deterioration and an accuracy of $+.1/-.4$ for low levels of engine deterioration, with deterioration defined in Appendix A. The variation, especially on the engine deterioration plot is rather large. For instance, a calculated engine deterioration level of .5 could indicate an actual engine deterioration anywhere from .2 - .9. Without measurement errors this variation would reduce to .3 - .75. It is

Measurement	Modifier
PS45	Recuperator Leakage
T6	Overall Engine Deterioration

Table 4.1: Set Up For Two Element SCAT

with these relatively poor results in mind that the steady-state iterative solutions were attempted.

4.2 Steady-State Iterative Solutions (SCAT)

Several different SCAT setups were attempted. The one that was settled on as being the most reliable in the face of the uncertainties outlined in Section 4.1 is a two element SCAT depicted in Table 4.1.

Remember, the SCAT augments the fundamental twelve element SLAM with extra measurements that are used to match modifiers in the cycle. SCAT works if the measurements are very well correlated with a modifier. It will be unreliable if the measurements are uncorrelated.

The results of the two element SCAT technique are presented in a similar manner to the open loop data and appear in Figure 4.3 and Figure 4.4.

We see a tighter variation in both the recuperator leakage and engine deterioration plots. Without measurement errors the SCAT technique works extremely well. However, realistic measurement errors must be assumed and these increase the variation to a similar level, although tighter, than the open loop algorithms.

The steady-state iterative solution (SCAT) can detect any leakage with an accu-

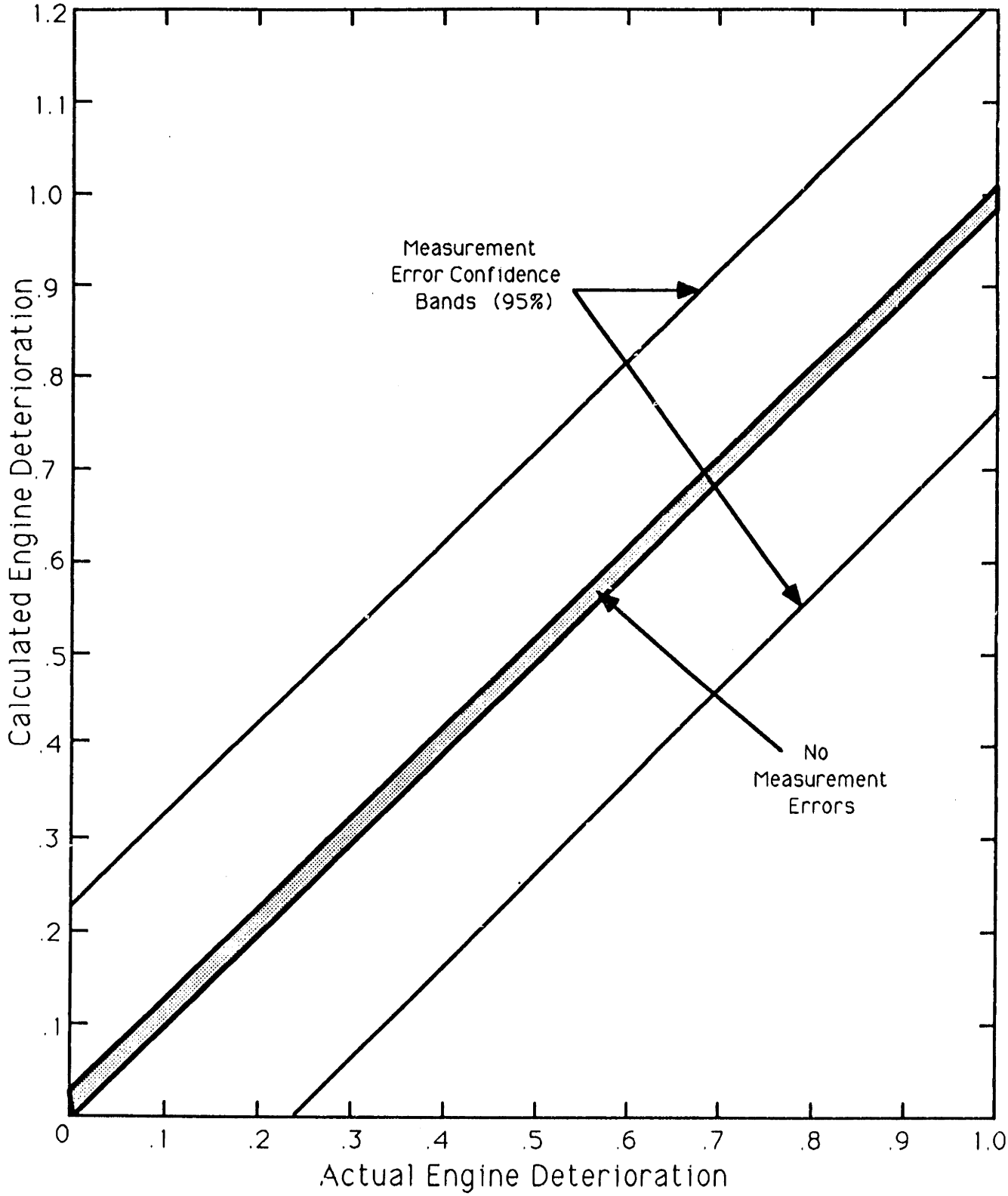

Figure 4.3: Calculated Engine Deterioration vs. Actual Engine Deterioration - SCAT

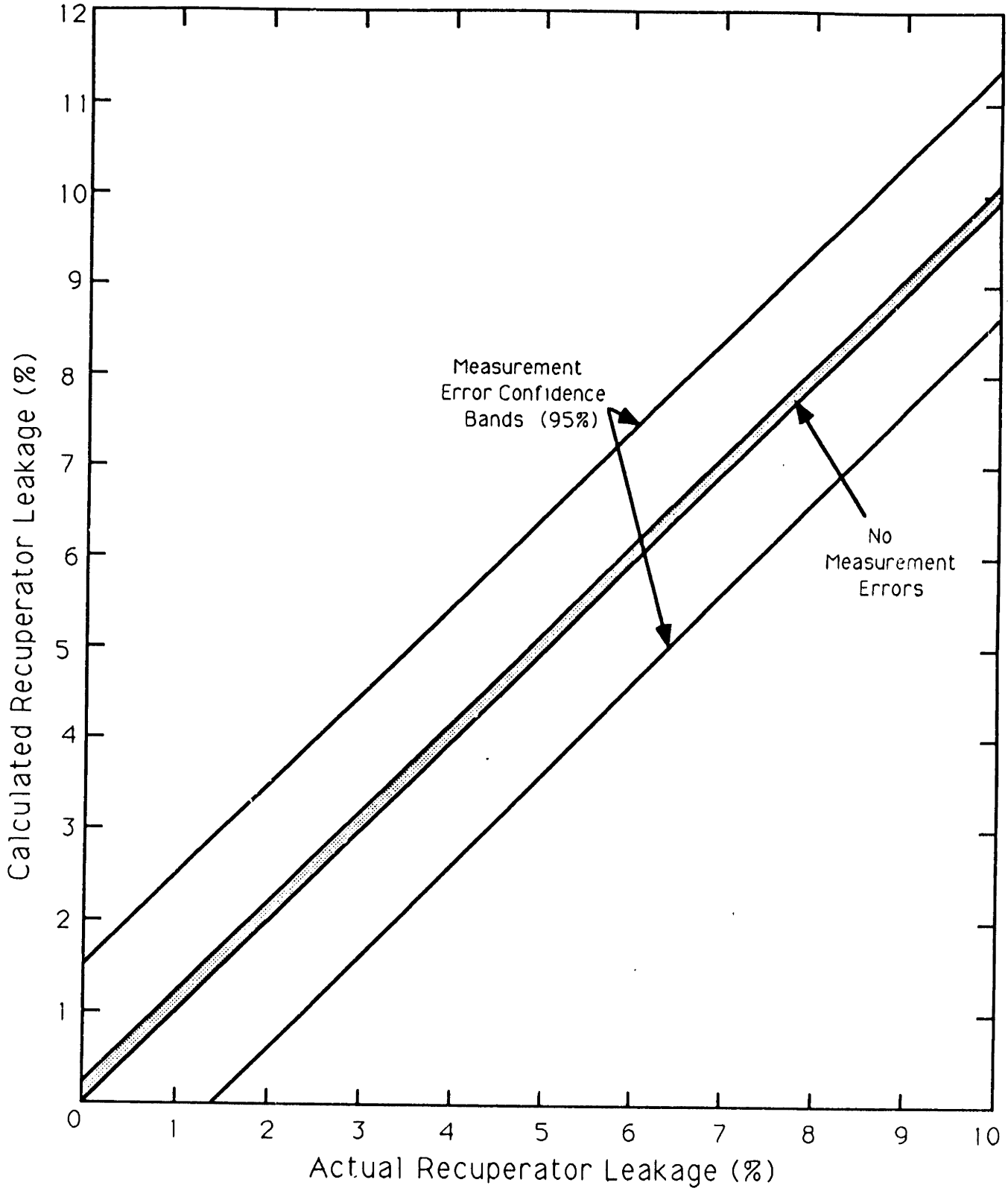

Figure 4.4: Calculated Recuperator Leakage vs. Actual Recuperator Leakage – SCAT

Diagnostic Algorithm	Range
Open Loop With Measurement Errors	.2 – .9
SCAT With Measurement Errors	.3 – .7
Open Loop Without Measurement Errors	.3 – .75
SCAT Without Measurement Errors	.48 – .52

Table 4.2: Comparison of Ranges for Detecting a Deterioration Level of .5 – Open Loop and SCAT

racy of ± 1.4 and engine deterioration with an accuracy of $\pm .22$, with deterioration defined in Appendix A. With no measurement errors this would be improved to nearly perfect detection of engine deterioration and recuperator leakage.

For a comparison of the two methods the results are superimposed and are plotted in Figure 4.5 and Figure 4.6.

These figures show that the two element SCAT is a more reliable method of determining engine deterioration and recuperator leakage than the open loop algorithms. For example, if the actual engine deterioration level was .5, the open loop algorithms could indicate a value anywhere from .2 – .9. The SCAT would improve this to anywhere from .3 – .7. Without measurement errors this would be improved from .3 – .75 to .48 – .52. This information is summarized in Table 4.2.

The slope of the curves in Figure 4.4 and Figure 4.3 are more near the ideal level of 1. For the open loop algorithms, the deterioration curve in particular has a slope less than 1, which increases the variation considerably. In addition, SCAT does not

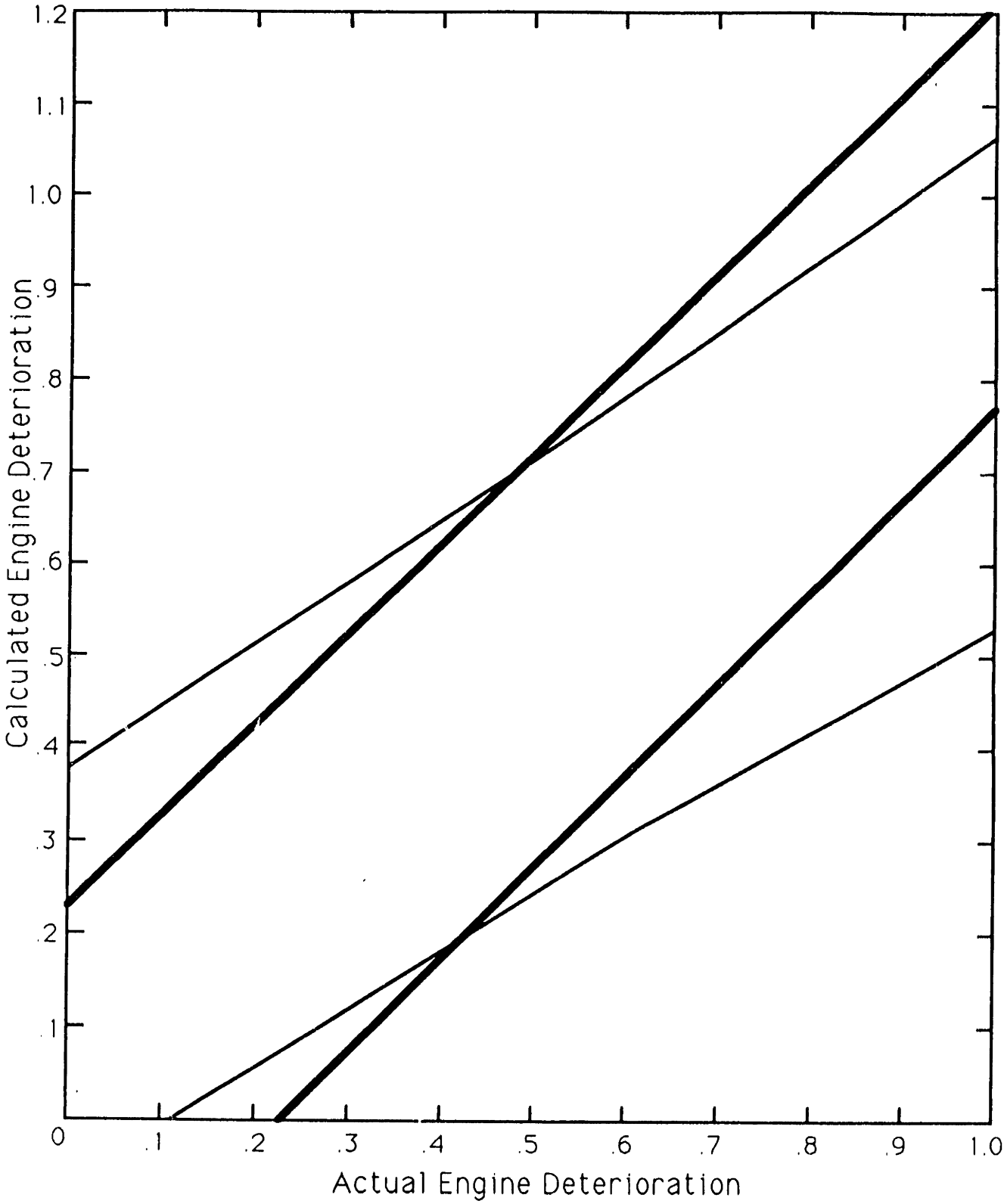

Figure 4.5: Calculated Engine Deterioration vs. Actual Engine Deterioration – Comparison of SCAT and Open Loop Algorithms

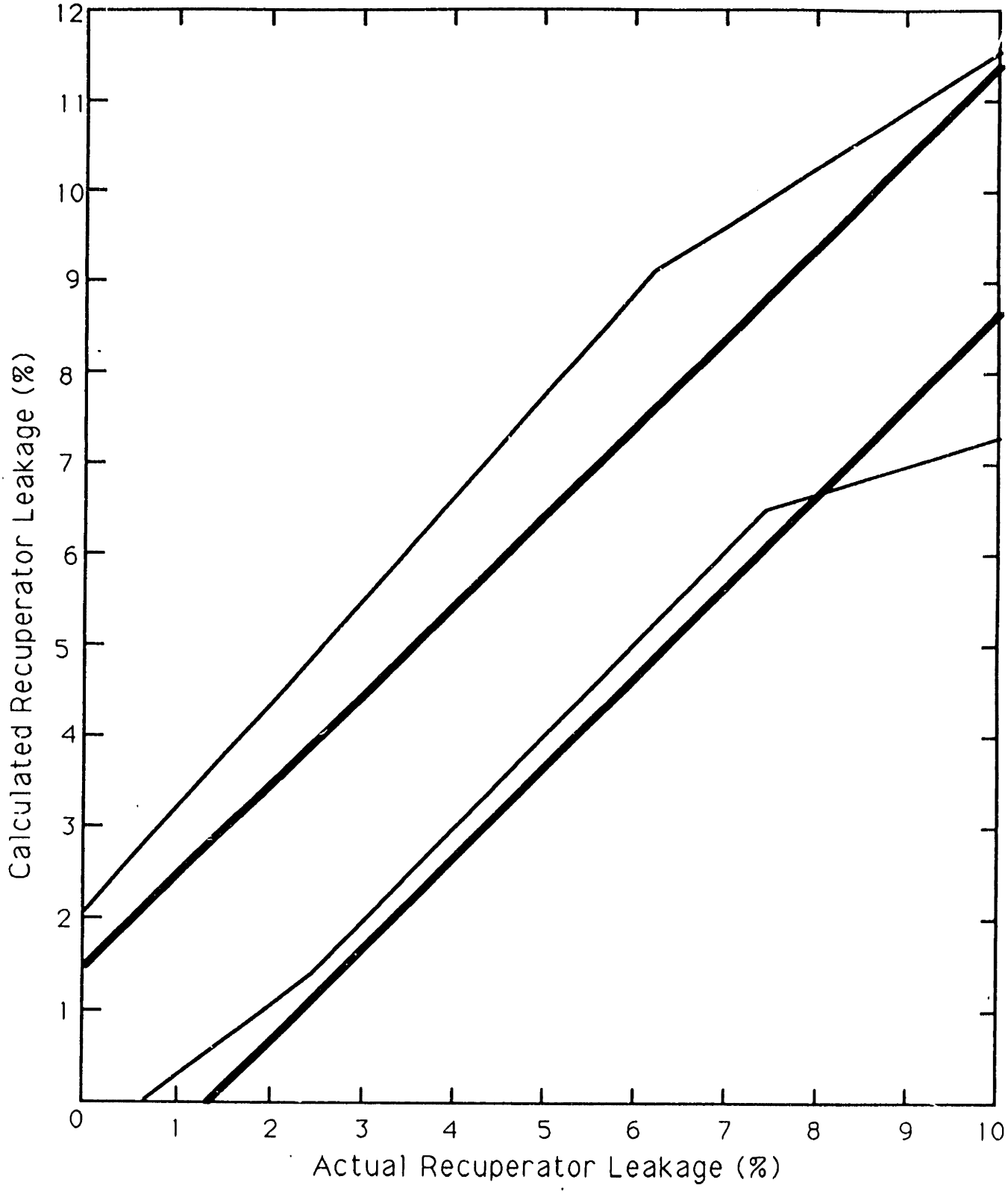

Figure 4.6: Calculated Recuperator Leakage vs. Actual Recuperator Leakage – Comparison of SCAT and Open Loop Algorithms

have to be performed at one study point but can be used anywhere in the operating envelope.

4.2.1 Other SCAT Approaches

Using just PS45 and T6 to do the SCAT analysis leaves two other measurements that are not being used. We still have T35 and PS31 which are extra sensed variables. It was hoped that these two variables could help us realize the secondary engine diagnostic goal of attempting to determine individual engine component health as opposed to an overall engine deterioration measure.

Since there are only four extra measurements we are limited to at maximum a four element SCAT. There are many different options with a two element, three element, and four element SCAT. The trick is to judiciously choose the model modifiers to match up to the measurements.

Several attempts were made to do this and they will be discussed briefly in this subsection. To choose the best SCAT set up available, each set up was subjected to the same test and the results were compared. The test consisted of

- Ability to detect a random pattern.
- Insensitivity to measurement errors.

The major problem of all of the three and four element SCAT setups was found to be sensitivity to measurement errors. Most of the SCAT setups attempted worked very well without measurement errors. However, when measurement errors are im-

posed on the system, the results are unreliable. Figures 4.7 – 4.16 demonstrate the effect of measurement errors on several different setups. The column of 2 σ values indicates 2 standard deviations. So for instance, in Figure 4.4, the value of $W_{\%leak}$ could be anywhere from 3.0 % ($5.0\% - 2\sigma$) to 7.0 % ($5.0 + 2\sigma$) with 95% confidence. The probability distribution is in the form of a Gaussian bell around the median value of 5%. The bell starts and ends at 3% and 7% respectively.

We can quickly see that, when the 2σ value gets to be large, the analysis is ineffective. For example, Figure 4.10 shows that the value for *Engdet* is centered around .495 but with measurement errors the gaussian bell extends from -.505 to 1.505. Clearly our value of *Engdet* could be anywhere in that area and is basically useless for adapting the T6 schedules.

In addition to T35 and PS31, some setups consider T3 as a possible measurement for this study. If T3 could be argued to be beneficial on a cost basis, then it could be included on the production engine. Each setup was subject to 50% engine deterioration and 5% recuperator leakage. The objective of each SCAT setup was to detect a 50% level of engine deterioration and 5% level of recuperator leakage. No SCAT could be found that could detect recuperator leakage reliably without PS45. This is the same result obtained with the open loop algorithms. If we want to be able to detect recuperator leakage, a PS45 measurement is required.

As is evidenced by these tables, with realistic measurement variations imposed on the system, any of the three and four element SCAT setups become unreliable.

Measurements	Cycle Parameters Modified	No Measurement Errors	Measurement Errors ($\pm 2\sigma$)
PS45	$W_{\%leak}$	5.0%	2.0%
T6	$\eta_{comp}, \eta_{hpt}, \eta_{lpt}, W_{cool}$ FF41,W2R,W26R	.499	.25

Figure 4.7: Two Element SCAT

Measurements	Cycle Parameters Modified	No Measurement Errors	Measurement Errors ($\pm 2\sigma$)
PS45	$W_{\%leak}$	5.0%	2.8%
T6	$\eta_{comp}, \eta_{hpt}, \eta_{lpt}$ $W_{cool}, W2R, W26R$	.501	.70
PS31	FF41	.495	.84

Figure 4.8: Three Element SCAT - $PS31 \Longrightarrow FF41$

Measurements	Cycle Parameters Modified	No Measurement Errors	Measurement Errors ($\pm 2\sigma$)
PS45	$W_{\%leak}$	5.1%	3.2%
T6	$\eta_{hpt}, \eta_{lpt}, W_{cool}$ FF41,W2R,W26R	.494	.83
T35	η_{comp}	.410	1.05

Figure 4.9: Three Element SCAT - $T35 \Longrightarrow \eta_{comp}$

Measurements	Cycle Parameters Modified	No Measurement Errors	Measurement Errors ($\pm 2\sigma$)
PS45	$W_{\%leak}$	5.0%	5.0%
T6	$\eta_{comp}, \eta_{lpt}, W_{cool}$ FF41,W2R,W26R	.495	1.10
PS31	η_{hpt}	.505	1.55

Figure 4.10: Three Element SCAT - $PS31 \Longrightarrow \eta_{hpt}$

Measurements	Cycle Parameters Modified	No Measurement Errors	Measurement Errors ($\pm 2\sigma$)
PS45	$W_{\%leak}$	5.0%	4.0%
T6	$\eta_{comp}, \eta_{lpt}, W_{cool}$ FF41,W2R,W26R	.484	1.45
PS31/PS45	η_{hpt}	.511	1.60

Figure 4.11: Three Element SCAT - $PS31/PS45 \Longrightarrow \eta_{hpt}$

Measurements	Cycle Parameters Modified	No Measurement Errors	Measurement Errors ($\pm 2\sigma$)
PS45	$W_{\%leak}$	5.0%	3.8%
T3	η_{comp}	.485	.62
PS31	η_{hpt}	.534	1.09

Figure 4.12: Three Element SCAT – No T6

Measurements	Cycle Parameters Modified	No Measurement Errors	Measurement Errors ($\pm 2\sigma$)
PS45	$W_{\%leak}$	5.0%	2.8%
T6	$\eta_{hpt}, \eta_{lpt}, W_{cool}$ W2R, W26R	.506	1.48
PS31	FF41	.502	1.07
T3	η_{comp}	.501	.96

Figure 4.13: Four Element SCAT – $PS31 \Longrightarrow FF41$

Measurements	Cycle Parameters Modified	No Measurement Errors	Measurement Errors ($\pm 2\sigma$)
PS45	$W_{\%leak}$	5.0%	1.0%
T6	η_{hpt}, η_{lpt}	.500	1.49
PS31	FF41	.497	1.01
T3	η_{comp}	.501	.95

Figure 4.14: Four Element SCAT – $T6 \Longrightarrow \eta_{hpt}, \eta_{lpt}$ only.

Measurements	Cycle Parameters Modified	No Measurement Errors	Measurement Errors ($\pm 2\sigma$)
PS45	$W_{\%leak}$	5.0%	2.4%
T6	η_{hpt}	.491	1.09
PS31	FF41	.502	1.20
T3	η_{comp}	.501	.410

Figure 4.15: Four Element SCAT – $T6 \Longrightarrow \eta_{hpt}$ only.

Measurements	Cycle Parameters Modified	No Measurement Errors	Measurement Errors ($\pm 2\sigma$)
PS45	$W_{\%leak}$	5.0%	4.2%
T6	$\eta_{hpt}, \eta_{lpt}, W_{cool}$	.498	1.65
PS31	FF41	.497	1.40
T3	η_{comp}	.502	.805

Figure 4.16: Four Element SCAT – $T6 \Longrightarrow \eta_{hpt}, \eta_{lpt}, W_{cool}$ only.

Measurement	Cycle Parameter Modified
FF41	Leakage Flow From Station 3
W2	Scaler on Mass Flow at Station 2
T25	Adder on η_{axial}
W26	Scaler on Corrected Flow at Station 26
T3	Adder on η_{cent}
P36	$\frac{\Delta P}{q}$ for duct from Station 35 to 36
P44	Adder on η_{hpt}
P31	$\frac{\Delta P}{q}$ for duct from Station 3 to 31
P3R	$\frac{\Delta P}{q}$ for duct from Station 31 to 3R
P35	$\frac{\Delta P}{q}$ for duct from Station 3R to 35
T35	Adder on T35

Table 4.3: SCAT Setup for Core Test

No close correlation could be found between the measurements and the scalers and adders on the system that would break apart the measure of engine deterioration. Relating T6 to an overall gauge of engine deterioration is the most robust in the face of measurement errors given the measurements available for use in this analysis.

The problem with attempting to do the SCAT in this manner is that the measurements are not directly correlated to any one or combination of cycle parameters. For example, the SCAT setup for the core test is depicted in Table 4.3.

The measurements are directly correlated to the parameter they modify. The duct dependent pressure losses are correlated to each pressure measurement along the way. It works well because of the constraints imposed on the system by the other

measurements and modifiers. The P31 measurement nails down the pressure loss in the duct leading to station 31. Since this is known, then the P3R measurement reliably nails down the pressure loss between station 31 and 3R. If P31 was not known, then correlating both pressure losses to P3R would not prove to be as accurate and reliable. This is the problem run into here trying to do SCAT on a production engine with limited measurements. Correlating PS31 to a scaler on FF41, or $\frac{PS31}{PS45}$ to η_{hpt}, makes sense physically if everything else in the system is constrained. However, there are not enough measurements to constrain the system satisfactorily. A difference in PS31 either due to measurement error or an actual physical difference does not reliably determine what is happening to FF41, because the system is not constrained adequately. When realistic system variations are assumed, the SCAT falls apart and basically gives unacceptable results.

However, tying all engine deterioration parameters to T6 does hold up adequately in the face of realistic system variations. This is not an ideal representation of engine deterioration since all efficiencies, etc. are forced to deteriorate in an identical manner. It is unlikely that the compressor and turbine will both lose exactly the same quantity of efficiency as the engine run time increases. However, it is certainly arguable that all components will deteriorate in a similar manner. Perhaps they will not deteriorate exactly the same but the overall engine will deteriorate in this fashion as run time increases. So, this representation of engine deterioration is indicative of physical reality althouhg perhaps it is not as flexible as one would like.

To conclude this section, a two element SCAT setup depicted in Table 4.1 gives the most robust results in the face of realistic system variation. Attempts to break up the overall engine deterioration vector into smaller components correlating to the other available measurements (PS31, T35, or possibly T3) were unsuccessful.

4.3 Automatic Update Scheme

As was discussed in Section 2.4 all of the engine thermodynamic limits (SM, T35, T41, T45) can be mapped into a single T6 schedule. The process of automatically updating the T6 schedule to reflect the engine and recuperator condition is the subject of this section.

The T6 schedule could be a single trivariate function of Ng, Np, and T1 where all of the limiting thermodynamic parameters are programmed into one table.

$$T6_{demand} = f(Ng, Np, T1)$$

However, it is more convenient to break the table into four separate tables reflecting each of the thermodynamic limits

$$T6_{SM} = f(Ng, Np, T1)$$

$$T6_{T35} = f(Ng, Np, T1)$$

$$T6_{T41} = f(Ng, Np, T1)$$

$$T6_{T45} = f(Ng, Np, T1)$$

and taking the minimum value to be the desired T6

$$T6_{demand} = min(T6_{SM}, T6_{T35}, T6_{T41}, T6_{T45}, T6_{limit})$$

This method of obtaining $T6_{demand}$ affords the ability to modify a single limit schedule without recomputing the entire schedule. It also suggests immediately which parameter is limiting.

In fact, due to hardware considerations, the on-line processor requires nothing more than bivariate functions. To achieve this the tables are collapsed by using corrected core speed ($\frac{Ng}{\sqrt{\theta_2}}$) instead of physical core speed and inlet temperature

$$T6_{SM} = f(\frac{Ng}{\sqrt{\theta_2}}, Np)$$

$$T6_{T35} = f(\frac{Ng}{\sqrt{\theta_2}}, Np)$$

$$T6_{T41} = f(\frac{Ng}{\sqrt{\theta_2}}, Np)$$

$$T6_{T45} = f(\frac{Ng}{\sqrt{\theta_2}}, Np)$$

$$T6_{demand} = min(T6_{SM}, T6_{T35}, T6_{T41}, T6_{T45}, T6_{limit})$$

The T6 tables could be expanded into quadvariate tables, if that were allowable. The matter of updating the T6 schedules would be reduced to precomputing quadvariate tables reflecting recuperator leakage and engine deterioration as well as corrected core speed and power turbine speed.

$$T6_{SM} = f(\frac{Ng}{\sqrt{\theta_2}}, Np, W_{\%leak}, Engdet)$$

$$T6_{T35} = f(\frac{Ng}{\sqrt{\theta_2}}, Np, W_{\%leak}, Engdet)$$

$$T6_{T41} = f(\frac{Ng}{\sqrt{\theta_2}}, Np, W_{\%leak}, Engdet)$$

$$T6_{T45} = f(\frac{Ng}{\sqrt{\theta_2}}, Np, W_{\%leak}, Engdet)$$

$$T6_{demand} = min(T6_{SM}, T6_{T35}, T6_{T41}, T6_{T45}, T6_{limit})$$

The values of $W_{\%leak}$ and $Engdet$ would have to be computed off line based on steady-state data. This would, in effect, be the automatic update of the schedules.

However, this is not possible due to the time constraint of quadvariate table lookups on-line. The T6 schedules must be recomputed off line and the old schedules should be replaced with new, reflecting the engine and recuperator health.

This is done by determining $W_{\%leak}$ and $Engdet$ from the SCAT analysis. Next, determine the new T6 schedules and scalers to be applied to old schedules from precast tables. For each point on the schedule defined by $\frac{Ng}{\sqrt{\theta_2}}$ and Np compute the original

schedules

$$T6_{SM} = f(\frac{Ng}{\sqrt{\theta_2}}, Np)$$

$$T6_{T35} = f(\frac{Ng}{\sqrt{\theta_2}}, Np)$$

$$T6_{T41} = f(\frac{Ng}{\sqrt{\theta_2}}, Np)$$

$$T6_{T45} = f(\frac{Ng}{\sqrt{\theta_2}}, Np)$$

and the new tables dependent on $Engdet$ and $W_{\%leak}$

$$ZT6_{SM} = f(\frac{Ng}{\sqrt{\theta_2}}, Np, W_{\%leak}, Engdet)$$

$$ZT6_{T35} = f(\frac{Ng}{\sqrt{\theta_2}}, Np, W_{\%leak}, Engdet)$$

$$ZT6_{T41} = f(\frac{Ng}{\sqrt{\theta_2}}, Np, W_{\%leak}, Engdet)$$

$$ZT6_{T45} = f(\frac{Ng}{\sqrt{\theta_2}}, Np, W_{\%leak}, Engdet)$$

then compute a scaler to make the transformation back and forth from the original to the updated schedules

$$ST6_{SM} = \frac{ZT6_{SM}}{T6_{SM}}$$

$$ST6_{T35} = \frac{ZT6_{T35}}{T6_{35}}$$

$$ST6_{T41} = \frac{ZT6_{T41}}{T6_{41}}$$

$$ST6_{T45} = \frac{ZT6_{T45}}{T6_{45}}$$

This scalers allow added flexibility in implementation of the schedules. One can simply adjust the scalers to implement the new schedules or switch back and forth from the old to the adapted schedules more freely with the use of the scalers.

Since this analysis is done off line, it is acceptable to use quadvariate table look-ups. The T6 schedules are replaced with the updated schedules at regular intervals during vehicle operation. Chapter 5 rehashes the adaptive update scheme and demonstrates the benefits in terms of gain in output horsepower of using the scheme.

Chapter 5

Benefits of Update Scheme

5.1 Outline of Update Scheme

As shown in Chapter 4, the two element SCAT provides the most reliable and robust determination of engine condition. This method is better than the open loop algorithms, all other three and four element SCAT's, and the dynamic tracking filter that was attempted. So basically, the task of automatically updating the T6 schedules breaks down into the following procedure:

1. Determine that the engine is at a steady-state condition (either GE/I or by collecting data over time and analyzing it).

2. Do SCAT analysis to determine *Engdet* and $W_{\%leak}$ (this might require a data reduction or averaging scheme to ascertain a single best value of *Engdet* and $W_{\%leak}$ given a number of measurements).

3. Generate new T6 schedules and scalers based on the values of *Engdet* and $W_{\%leak}$.

4. Implement new schedules into control system hardware.

This analysis would be done off line although it could be done on board the vehicle by a processor that is not in the loop.

5.2 Testing of Algorithm

Several known engine deteriorations and leakages were input. They were ascertained by the SCAT analysis and new schedules were generated. At this point three runs were made to demonstrate the advantages of the new schedules.

1. Run with original schedules to determine horsepower loss due to leakage and/or deterioration.

2. Run with new schedules to compare horsepower loss with amount lost with the original schedules.

3. Run with ideal control to determine the unavoidable horsepower loss necessary to avoid violating thermodynamic limits.

The ideal control affords the valuable capability of running the engine so that it is always operating at a thermodynamic limit. This allows us to see what horsepower loss is unavoidable, since all thermodynamic limits must remain satisfied even with

the engine deterioration and recuperator leakage. The runs with the new schedules should be significantlyu closer to the value of output horsepower obtained with the ideal control than the runs with the original schedules.

To illustrate the effectiveness of the algorithm several conditions will be investigated in detail.

5% Recuperator Leakage

The first instance is the condition of no engine deterioration and 5% recuperator leakage. Figure 2.9 indicates that this condition results in 17.7% horsepower loss at maximum power using the original tables. 9.8% of this is unavoidable and would result if the engine were still operating at some thermodynamic limit. Therefore, if the update scheme was ideal, then this 17.7% loss would be reduced to a 9.8% loss in output horsepower.

To test this the procedure outlined above was used and the new tables were generated. Using the new tables the output horsepower loss was reduced to 11.9%. Therefore, in this instance, a 5.8% gain in output horsepower results from adapting the schedules. The maximum possible gain was 7.9%.

It is important to check to see if any thermodynamic limits were violated using the new schedules. This could happen if the engine deteriorates in some non-standard way, for instance, the compressor deteriorates completely but the turbine remains at nominal levels. The value of *Engdet* would be somewhere in between 0 and 1 and the new schedules would not reflect the poor compressor performance explicitly. This

Control Used	Output Horsepower Loss at Maximum Power (%)	Output Horsepower Loss at Intermediate Power (%)
Nominal Schedules	17.7	10.6
Adapted Schedules	11.9	7.9
Ideal Control	9.8	7.2

Table 5.1: Horsepower Loss for 5% Recuperator Leakage

might allow a thermodynamic limit to be violated such as T35 or SM2W or SM26W even though the other thermodynamic limits are satisfied. This is why it would have been advantageous to be able to explicitly determine component performance levels. For a simple case such as this, violating a thermodynamic limit is not a problem.

The results for this condition are summarized in Table 5.1. An intermediate power point is included in Table 5.1 for comparison. We see that, at this power setting, we recover 2.7% out of a possible 3.4% of output horsepower. This would allow significant fuel savings over the life of the engine.

The most interesting figures are the ones for maximum output horsepower. This relates to overall peak performance capabilities of the vehicle. At intermediate power settings, the vehicle commander will simply use a higher setting to attain the desired output as the engine deteriorates. However, this is not the most efficient operation of the vehicle and will result in wasted fuel. The adaptive algorithms will provide better fuel efficiency at intermediate power levels in addition to increased maximum output horsepower.

Control Used	Output Horsepower Loss at Maximum Power (%)
Nominal Schedules	26.2
Adapted Schedules	18.7
Ideal Control	13.8

Table 5.2: Horsepower Loss for Level 1 Engine Deterioration

Fully Deteriorated Engine

This test involved subjecting the engine to a level 1 engine deterioration (see Appendix A) with no recuperator leakage. Figure 2.9 indicates that this condition results in 26.2% horsepower loss at maximum power using the original tables. 13.8% of this is necessary to avoid violating any thermodynamic limits.

New T6 schedules were generated using the values of *Engdet* and $W_{\%leak}$ obtained from the SCAT analysis. Using the new tables, the horsepower loss was reduced to 18.7%. So the adaptive algorithm recovered 7.5% of a possible 12.4% of output horsepower in this instance. Once again, no thermodynamic limits were violated with the new schedules. The results for this condition are summarized in Table 5.2.

Level .5 Deterioration with 5% Recuperator Leakage

This test involved subjecting the engine to a level .5 engine deterioration with 5% recuperator leakage. Figure 2.9 indicates that this condition results in 32.7% horsepower loss at maximum power using the original tables. 18.4% of this is necessary

Control Used	Output Horsepower Loss at Maximum Power (%)
Nominal Schedules	32.7
Adapted Schedules	24.4
Ideal Control	18.4

Table 5.3: Horsepower Loss for Level .5 Engine Deterioration and 5% Recuperator Leakage

to avoid violating thermodynamic limits. This figure was obtained using the ideal control.

Once again new T6 schedules were generated using the values of *Engdet* and $W_{\%leak}$ obtained from the two element SCAT analysis. The new tables reduced the horsepower loss to 24.4%. In this instance the adaptive algorithm recovered 8.3% of a possible 14.3% of maximum output horsepower. The results for this condition are summarized in Table 5.3.

Tables of Results

This procedure was repeated for several other conditions and some of the results are summarized in the Table 5.4 - Table 5.8.

All of these tables show basically the same positive result: The adaptive algorithm greatly increases maximum power available in the face of engine deterioration and recuperator leakage. This is contingent on accurately identifying recuperator leakage and engine deterioration so as to make sure not to violate any of the thermodynamic

Control Used	Output Horsepower Loss at Maximum Power (%)
Nominal Schedules	41.0
Adapted Schedules	27.0
Ideal Control	25.2

Table 5.4: Horsepower Loss for 10% Recuperator Leakage

Control Used	Output Horsepower Loss at Maximum Power (%)
Nominal Schedules	34.5
Adapted Schedules	23.1
Ideal Control	19.7

Table 5.5: Horsepower Loss for .25 Engine Deterioration and 7% Recuperator Leakage

limits in the engine.

5.3 Effect of Measurement Errors

As Figure 4.3 and Figure 4.4 show, the measurement errors introduce a variation related to the standard deviations of *Engdet* and $W_{\%leak}$. These are a result of the uncertainty of the sensors used to extract information from the engine. This range on the values of *Engdet* and $W_{\%leak}$ could cause an inaccurate update of the schedules. This could result in a steady-state thermodynamic limit being violated when the new T6 schedules are used. In order to test this several runs were made. These

Control Used	Output Horsepower Loss at Maximum Power (%)
Nominal Schedules	31.2
Adapted Schedules	21.3
Ideal Control	17.3

Table 5.6: Horsepower Loss for .75 Engine Deterioration and 3% Recuperator Leakage

Control Used	Output Horsepower Loss at Maximum Power (%)
Nominal Schedules	19.5
Adapted Schedules	12.3
Ideal Control	9.4

Table 5.7: Horsepower Loss for .75 Engine Deterioration and no Recuperator Leakage

Control Used	Output Horsepower Loss at Maximum Power (%)
Nominal Schedules	9.0
Adapted Schedules	6.3
Ideal Control	5.1

Table 5.8: Horsepower Loss for no Engine Deterioration and 3% Recuperator Leakage

	Output Horsepower Loss at Maximum Power (%)	Thermodynamic Limits Violated
Ideal Control	5.1	none
Original Schedules	9.0	none
$+2\sigma$	3.5	T45
Nominal Adaptive Schedules	6.3	none
-2σ	7.9	none

Table 5.9: Effect of Measurement Errors for no Engine Deterioration and 3% Recuperator Leakage.

involved running a known condition such as level .5 engine deterioration and 5% recuperator leakage. Then, since the bounds were obtained on *Engdet* and $W_{\%leak}$ from the Monte Carlo simulations done with the SCAT analysis, we used these upper and lower bounds to obtain two other sets of possible tables for this same condition. These represent the two extreme sets of tables that could be generated for a given condition. The results obtained from these two sets of tables give the bounds on the maximum output horsepower variations for a given deteriorated condition. It is important to see that the thermodynamic limits remain satisfied with maximum measurement error effects included.

Several points were analyzed in this fashion and the results are summarized in Table 5.9 - Table 5.15.

Table 5.9 - Table 5.15 indicate that a bias needs to be put on the new T6 schedules to avoid violating thermodynamic limits. In most cases, when the worst possible measurement errors are assumed ($+2\sigma$), a thermodynamic limit is violated. This

	Output Horsepower Loss at Maximum Power (%)	Thermodynamic Limits Violated
Ideal Control	9.8	none
Original Schedules	17.7	none
$+2\sigma$	6.7	T41, T45
Nominal Adaptive Schedules	11.9	none
-2σ	13.8	none

Table 5.10: Effect of Measurement Errors for no Engine Deterioration and 5% Recuperator Leakage.

	Output Horsepower Loss at Maximum Power (%)	Thermodynamic Limits Violated
Ideal Control	13.8	none
Original Schedules	26.2	none
$+2\sigma$	13.0	T45
Nominal Adaptive Schedules	18.7	none
-2σ	21.3	none

Table 5.11: Effect of Measurement Errors for Level 1 Engine Deterioration and no Recuperator Leakage.

	Output Horsepower Loss at Maximum Power (%)	Thermodynamic Limits Violated
Ideal Control	18.4	none
Original Schedules	32.7	none
$+2\sigma$	16.5	T41, T45
Nominal Adaptive Schedules	24.4	none
-2σ	27.1	none

Table 5.12: Effect of Measurement Errors for Level .5 Engine Deterioration and 5% Recuperator Leakage.

	Output Horsepower Loss at Maximum Power (%)	Thermodynamic Limits Violated
Ideal Control	19.7	none
Original Schedules	34.5	none
$+2\sigma$	18.0	T45
Nominal Adaptive Schedules	23.1	none
-2σ	27.2	none

Table 5.13: Effect of Measurement Errors for Level .25 Engine Deterioration and 7% Recuperator Leakage.

	Output Horsepower Loss at Maximum Power (%)	Thermodynamic Limits Violated
Ideal Control	17.3	none
Original Schedules	31.2	none
$+2\sigma$	16.0	T41, T45
Nominal Adaptive Schedules	21.3	none
-2σ	24.1	none

Table 5.14: Effect of Measurement Errors for Level .75 Engine Deterioration and 3% Recuperator Leakage.

	Output Horsepower Loss at Maximum Power (%)	Thermodynamic Limits Violated
Ideal Control	9.4	none
Original Schedules	19.5	none
$+2\sigma$	9.0	T45
Nominal Adaptive Schedules	12.3	none
-2σ	14.1	none

Table 5.15: Effect of Measurement Errors for Level .75 Engine Deterioration and no Recuperator Leakage.

	Output Horsepower Loss at Maximum Power (%)	Thermodynamic Limits Violated
Ideal Control	5.1	none
Original Schedules	9.0	none
$+2\sigma$	5.1	none
Nominal Adaptive Schedules	6.9	none
-2σ	8.2	none

Table 5.16: Effect of Measurement Errors for no Engine Deterioration and 3% Recuperator Leakage - Biased Tables

limit is usually T45 or T41. Although this worst possible scenario is unlikely to occur it is important that under no circumstances are the steady-state thermodynamic cycle limits violated. To alleviate this a bias must be put on the new T6 schedules. An analysis was done to determine the smallest bias required to insure that no limits were violated. This bias was applied to the schedules when they are created off line and the preceding analysis was repeated. It is important to see that the bias does not overwhelm the performance gains made available by the update scheme. Table 5.16 - Table 5.22 summarize the results using the new biased tables.

The results summarized in Table 5.16 - Table 5.22 are very encouraging. They show significant performance gains for even the worst possible measurement error scenario. The bias that is necessary to protect thermodynamic limits does not overwhelm the gains made available by the update scheme, although it does diminish them somewhat. No thermodynamic limits are violated under the worst possible measurement error scenario ($+2\sigma$). In addition, there are still significant performance improvements

	Output Horsepower Loss at Maximum Power (%)	Thermodynamic Limits Violated
Ideal Control	9.8	none
Original Schedules	17.7	none
$+2\sigma$	9.8	none
Nominal Adaptive Schedules	13.6	none
-2σ	15.0	none

Table 5.17: Effect of Measurement Errors for no Engine Deterioration and 5% Recuperator Leakage - Biased Tables

	Output Horsepower Loss at Maximum Power (%)	Thermodynamic Limits Violated
Ideal Control	13.8	none
Original Schedules	26.2	none
$+2\sigma$	17.1	none
Nominal Adaptive Schedules	20.6	none
-2σ	22.1	none

Table 5.18: Effect of Measurement Errors for Level 1 Engine Deterioration and no Recuperator Leakage - Biased Tables

	Output Horsepower Loss at Maximum Power (%)	Thermodynamic Limits Violated
Ideal Control	18.4	none
Original Schedules	32.7	none
$+2\sigma$	20.0	none
Nominal Adaptive Schedules	26.2	none
-2σ	29.2	none

Table 5.19: Effect of Measurement Errors for Level .5 Engine Deterioration and 5% Recuperator Leakage - Biased Tables

	Output Horsepower Loss at Maximum Power (%)	Thermodynamic Limits Violated
Ideal Control	19.7	none
Original Schedules	34.5	none
$+2\sigma$	20.5	none
Nominal Adaptive Schedules	24.9	none
-2σ	28.0	none

Table 5.20: Effect of Measurement Errors for Level .25 Engine Deterioration and 7% Recuperator Leakage – Biased Tables

	Output Horsepower Loss at Maximum Power (%)	Thermodynamic Limits Violated
Ideal Control	17.3	none
Original Schedules	31.2	none
$+2\sigma$	18.1	none
Nominal Adaptive Schedules	23.0	none
-2σ	25.7	none

Table 5.21: Effect of Measurement Errors for Level .75 Engine Deterioration and 3% Recuperator Leakage – Biased Tables

	Output Horsepower Loss at Maximum Power (%)	Thermodynamic Limits Violated
Ideal Control	9.4	none
Original Schedules	19.5	none
$+2\sigma$	9.9	none
Nominal Adaptive Schedules	13.3	none
-2σ	15.0	none

Table 5.22: Effect of Measurement Errors for Level .75 Engine Deterioration and no Recuperator Leakage – Biased Tables

with the worst possible measurement errors (-2σ) as well.

5.4 Effect of VATN Saturation

The level of T6 is controlled by opening and closing the VATN. If the desired T6 is higher that the present level, the VATN is closed down to increase pressure on the system and to raise T6. If the desired T6 is lower than the present level, the VATN is opened to relieve pressure on the system and lower T6 to the desired level.

When the VATN saturates by hitting its physical limit, it is no longer effective in controlling T6. At high power deteriorated points it saturates wide open. This implies that T6 is too high and some thermodynamic limit is being violated. To compensate for this the gas generator speed is dropped to lower the overall system energy and to bring T6 to its desired level. This, of course, lowers the output horsepower available but maintains the engine operating at safe levels.

Therefore, the control system attains the desired T6 by opening and closing the VATN to the proper level. If the VATN saturates before the desired T6 level is reached, the gas generator speed is then dropped to obtain the desired T6.

Under no circumstances are thermodynamic limits to be violated at steady-state. So although the VATN might saturate, the control system compensates by dropping gas generator speed to keep the engine operating at safe levels.

Chapter 6

Conclusions and Recommendations

6.1 Conclusions

In this thesis a method is developed which will automatically adapt the control schedules of a regenerative turboshaft engine woth a variable area turbine nozzle. This was undertaken to alleviate unacceptable performance loss that occurs when the engine deteriorates under field conditions.

For the engine studied in this thesis, all limiting thermodynamic parameters are scheduled open loop for a value of T6. When the engine deteriorates under field conditions, performance losses can be significant due to the inherent bias created by scheduling all engine limits open loop with T6. The engine is running to a nominal

value of T6 which assumes a nominal engine. When the engine deteriorates, the limiting parameters change over the operating envelope and the T6 schedule must change to reflect the new engine condition.

In order to adapt the schedules, the engine condition must be known. This is the main analytical portion of this work. Two apporaches were undertaken to evaluate engine condition. The selected method was a two element SCAT analysis of steady-state data. This analysis gives an indication of overall engine deterioration, *Engdet*, and a measure of recuperator leakage, $W_{\%leak}$. New schedules are generated out of the loop and inserted in the control system hardware based on these two parameters.

Specific conclusions are:

- Two element SCAT provides the most robust indication of engine and recuperator health.
- The adaptive T6 schedules recover, on the average, 65% of available horsepower that is lost due to engine deterioration and recuperator leakage.
- Performance loss due to recuperator leakage can be separated adequately from performance loss due to engine deterioration.

6.2 Recommendations for Further Study

Through the course of this work many interesting ideas and directions were discussed which had to be abandoned due to time considerations. Some of these could be

investigated in detail and the results coulud provide a more flexible, robust adaptive update scheme.

Averaging Scheme and Steady-State Determination

A reliable method of determining if the engine is at steay-state is necessary to do this analysis. This could involve simply monitoring key parameters over time to check if they are within a tolerance. More analysis needs to be done, possibly with engine test data, to determine when the engine is at steady-state over the operating envelope so data can be collected for analysis.

In addition, some sort of averaging or filtering scheme will need to be employed before using the data. Either the string of measurements could be reduced or the results of numerous SCAT analyses on a string of measurements could be reduced. The end result of the SCAT analysis must be a single set of values for *Engdet* and $W_{\%leak}$. More work needs to be done to determine how to reduce the data into a single number so the schedules can be updated. Once again, engine test data may prove helpful for this task.

Iterative Open Loop Algorithms

The determination of *Engdet* depends on the calculation of $W_{\%leak}$ in the chosen open loop algorithm. *Engdet* has a very large variation in part because of the dependence on $W_{\%leak}$. An interesting idea would be to go back to the original algorithms and iterate on them to produce a better indication of *Engdet* and $W_{\%leak}$.

Since the operating line of the engine migrates with deterioration and leakage, the open loop aerothermal correlation could be made a function of these two parameters as well. The first time through, a leakage of 0% and an engine deterioration level of 0 would be assumed. After the first pass we would have a value for these two parameters and the algorithms would attempt to iterate and converge on a more accurate value. This would require a significant effort as the correlations would have to be expanded to include *Engdet* and $W_{\%leak}$. This would be a tricky scheme but could provide more accurate results if it turned out to be well behaved.

Dynamic Update

As Section 4.2 shows, the two element SCAT approach gives the best results in the face of measurement uncertainty and engine to engine variation. A problem with using SCAT is that it is a steady-state analysis and as such the data must be acquired at steady-state. This raises the complication of making sure the engine is at steady-state when the analysis is done. This engine rarely operates at steady-state with the thermal and volumetric lags introduced by the recuperator and the power turbine speed fluctuations. Certain conditions, such as GE/I would provide a steady-state point but in general the engine is not at steady-state. Of course, the engine could be forced to be at steady-state for the purposes of this analysis, but if a dynamic method could accomplish the same results it would be more desirable.

A constant gain extended Kalman tracking filter was attempted in [Chi85] for a turbofan engine. It was concluded that it cannot be used to track component efficiency

trends. The reason is that implementation of the filter requires that the state vector be augmented with the extra measurements that are not required to define the cycle. Therefore, no reliable nominal points can be determined around which to linearize the system. The extra measurements, PS45 and T6, will not have a nominal value around which to linearize since they are variable depending on the particular cycle.

A dynamic update scheme would increase the versatility of the system. It would be a worthwhile area of research into a solution for the problem investigated in this thesis.

Engdet and $W_{\%leak}$ Over the Operating Envelope

It is possible that the amount of engine deterioration and recuperator leakage will vary depending on the operating condition. A more sophisticated model of engine deterioration and recuperator leakage which includes variations over the oeprating regime may need to be employed upon further analysis. Although taking recuperator leakage to be a straight percentage of flow entering the recuperator certainly seems reasonable, a more complex model of recuperator leakage may provide more insight and be more accurate. This model could be based on the physics in the recuperator or could be obtained by analyzing test data.

Test Data

Another potentially rich area of study is to analyze the update scheme using engine test data. This would introduce real measurement and process uncertainty into the

analysis. This is a demonstrator engine program and is still under development. As such, there is no test data available to analyze yet. However, in the near future, it would be very interesting to actually test out this engine diagnostic scheme on a physical engine.

Bibliography

[Chi85] Mei F. Chiu. Tracking filter for an embedded real time turbofan engine model. Master's thesis, MIT, 1985.

[Gel74] Arthur Gelb, editor. *Applied Optimal Estimation.* MIT Press, 1974.

[KM87] Kate Koenig and Wayne Miller. Regenerative engine controls. Internal GE document, 1987. IR&D Report, Project 9.45.

[KM88] Kate Koenig and Wayne Miller. Regenerative engine controls. Internal GE document, 1988. IR&D Report, Project 9.45.

[KM89] Kate Koenig and Wayne Miller. Regenerative engine controls. Internal GE document, 1989. IR&D Report, Project 9.45.

[Ort82] Paul Ortiz. Applied engine performance analysis. Internal GE document, 1982.

[Pin85] Fred J. Pineo. Adaptive update method for embedded real time jet engine model. Master's thesis, MIT, 1985.

Appendix A

Engine Deterioration Definition

A fully deteriorated engine is defined as:

- -2 points on η_{axial}
- -1.5% on axial compressor flow function
- -2 points on η_{cent}
- -1.5% on centrifugal compressor flow function
- -2 points on η_{hpt}
- -2 points on η_{lpt}
- $+1.5\%$ on power turbine flow function
- $+\frac{1}{4}\%$ on all cooling flows

An engine deteriorated to this level is considered fully deteriorated. All other deterioration conditions are represented by a number ranging from 0 to 1. A deterioration level of 0 represents a nominal engine. A deterioration level of 1 represents a fully deteriorated engine.

Appendix B

Measurement Error Definitions

The measurement errors imposed on the system are representative of realistic sensor accuracies available for the production engine. They were defined as follows for the Monte Carlo simulations:

Sensed Variable	Standard Deviations
T2	5.0 deg
T35	10.0 deg
T6	15.0 deg
P2	.1 % of point
PS31	.1 % of point
PS45	.15 % of point
XNg	.0135 %
XNp	.0135 %
VATN	4 % of stroke

Table B.1: Measurement Error Definitions